energies

MDPI

Article

Evaluation of a Simplified Model for Three-Phase Equilibrium Calculations of Mixed Gas Hydrates

Panagiotis Kastanidis [1,2], George E. Romanos [1], Athanasios K. Stubos [3], Georgia Pappa [2], Epaminondas Voutsas [2] and Ioannis N. Tsimpanogiannis [4,*]

[1] Institute of Nanoscience and Nanotechnology, National Center for Scientific Research "Demokritos", Aghia Paraskevi, 15310 Athens, Greece
[2] Laboratory of Thermodynamics and Transport Phenomena, School of Chemical Engineering, National Technical University of Athens, 9 Heroon Polytechniou Str., Zografou Campus, 15780 Athens, Greece; evoutsas@chemeng.ntua.gr (E.V.)
[3] Environmental Research Laboratory, National Center for Scientific Research "Demokritos", 15310 Aghia Paraskevi Attikis, Greece; stubos@ipta.demokritos.gr
[4] Chemical Process & Energy Resources Institute (CPERI), Centre for Research & Technology Hellas (CERTH), 57001 Thessaloniki, Greece
* Correspondence: i.n.tsimpanogiannis@certh.gr

Abstract: In this study, we perform an extensive evaluation of a simple model for hydrate equilibrium calculations of binary, ternary, and limited quaternary gas hydrate systems that are of practical interest for separation of gas mixtures. We adopt the model developed by Lipenkov and Istomin and analyze its performance at temperature conditions higher than the lower quadruple point. The model of interest calculates the dissociation pressure of mixed gas hydrate systems using a simple combination rule that involves the hydrate dissociation pressures of the pure gases and the gas mixture composition, which is at equilibrium with the aqueous and hydrate phases. Such an approach has been used extensively and successfully in polar science, as well as research related to space science where the temperatures are very low. However, the particular method has not been examined for cases of higher temperatures (i.e., above the melting point of the pure water). Such temperatures are of interest to practical industrial applications. Gases of interest for this study include eleven chemical components that are related to industrial gas-mixture separations. Calculations using the examined methodology, along with the commercial simulator CSMGem, are compared against experimental measurements, and the range of applicability of the method is delineated. Reasonable agreement (particularly at lower hydrate equilibrium pressures) between experiments and calculations is obtained considering the simplicity of the methodology. Depending on the hydrate-forming mixture considered, the percentage of absolute average deviation in predicting the hydrate equilibrium pressure is found to be in the range 3–91%, with the majority of systems having deviations that are less than 30%.

Keywords: gas hydrates; hydrate equilibrium pressure; gas-mixture separation

Citation: Kastanidis, P.; Romanos, G.E.; Stubos, A.K.; Pappa, G.; Voutsas, E.; Tsimpanogiannis, I.N. Evaluation of a Simplified Model for Three-Phase Equilibrium Calculations of Mixed Gas Hydrates. *Energies* **2024**, *17*, 440. https://doi.org/10.3390/en17020440

Academic Editors: Parisa Naeiji and Judith Schicks

Received: 24 November 2023
Revised: 5 January 2024
Accepted: 10 January 2024
Published: 16 January 2024

1. Introduction

Under conditions of low temperatures or high pressures, water molecules can self-assemble in forming three-dimensional crystalline structures that contain cavities/cages. These cavities can be stabilized if a fraction (i.e., rendering hydrate non-stoichiometric materials) of them, which belong to the hydrate crystal unit cell, are occupied by certain types of guest molecules that have an appropriate size to fit within them (e.g., CH_4, CO_2, N_2, etc.). Such ice-like, solid materials are known as clathrate hydrates or simply "hydrates" [1–3].

Hydrates are very important compounds due to their involvement in a number of major energy-related industrial [4–8] and environmental [9,10] applications. Depending on

the particular application, the appearance/formation of hydrates can be seen either as a major nuisance or as acting beneficially for the process of interest.

For example, hydrate formation is a major concern for safety and flow assurance in gas/oil pipelines [11–13], as well as unit operations where pressure and temperature conditions exist, such that hydrate formation is possible [3]. Significant effort and financial resources are dedicated in order to either completely avoid hydrate formation or to effectively control hydrate formation and the subsequent hydrate particle agglomeration. In a related context, during oil/gas exploration/exploitation operations, drilling through hydrate layers requires special care, since uncontrolled hydrate dissociation can be the cause of serious industrial accidents [14,15].

On the other hand, the hydrate characteristic to incorporate/store large volumes of gases within the hydrate crystal can be beneficial. In particular, hydrates are studied as a possible source of energy [4–7], since an enormous amount of carbon is deposited in worldwide accumulations of hydrates, containing predominantly methane, both on-shore (under the permafrost), and off-shore (in marine sediments). The recoverable amount of methane is, however, an issue that is currently under debate [16–18]. Methane production from the dissociation of hydrates confined within marine sediments requires a better understanding of the interactions between the dissociation thermodynamics occurring under different types of confinement, hydrate saturations, and the different production schemes (i.e., depressurization, thermal stimulation, hydrate inhibitor injection) [19–23]. Significant challenges need to be addressed in an adequate manner in order to incorporate hydrate deposits into the future energy mix in use [7,24]. Furthermore, hydrates can be used for storage and transportation of "energy carrier" gases (e.g., methane [25,26], hydrogen [27–29]). The characteristic of hydrates to selectively incorporate gases in their solid structure has been considered in order to achieve gas-mixture separation [30–33]. Similarly, the exclusion of ions from the hydrate crystals makes the use of hydrate-based technologies attractive for water desalination as well [34,35].

The particular aspect of hydrates to selectively incorporate gases in their solid structure and its use in hydrate-based applications for gas-mixture separations is the main focus of the current study. In order to design gas-mixture separation processes, such as natural gas purification or CO_2 capture from flue-gas streams that are based on hydrates, accurate thermodynamic, transport, and kinetic properties are required for all the involved pure components and their mixtures [8]. As discussed extensively in [36,37], there are three major approaches that have been employed in order to obtain such properties, namely, (i) experimental measurements, (ii) atomistic scale simulations, and (iii) continuum-scale theories. It should be noted that each one of the approaches for property estimation has advantages and disadvantages, including the following:

(i) When fluid mixtures are involved, performing experiments that consider all the possible mixture compositions can be significantly expensive and time-consuming. Therefore, it is of utmost importance to develop alternative thermodynamic tools that can be used to calculate the required properties of the pure components and their mixtures. Such are the cases of atomistic scale simulations, and the models based on continuum-scale theories.

(ii) Molecular simulations (e.g., Molecular Dynamics [38–46] or Monte Carlo [47–57] simulations) can use very detailed physics at the microscopic level; however, they are very computationally demanding, and therefore, the size of the system under consideration is very small, and the considered times are usually short (e.g., up to several microseconds). Therefore, such types of simulations are hard to use during process design or process-optimization schemes.

(iii) Models based on continuum-scale (macroscopic) theories, which are related to hydrate-forming systems, include those developed for the calculation of the three-phase (Hydrate–Liquid water–Vapor; H–L_w–V) equilibrium pressure and temperature conditions via a methodology that couples the van der Waals and Platteeuw statistical theory [58] with an Equation of State (EoS) [59–64]. The particular coupling is con-

sidered as one of the best examples of the application of Statistical Thermodynamic Theory toward the solution of a real industrial problem. Parrish and Prausnitz [59] pioneered the earlier development of the methodology, and an extensive review of the earlier studies was provided by Holder et al. [61] and Englezos [65]. While a significant number of studies considered the use of cubic EoS [59–62,66–70], during recent years, non-cubic EoS (e.g., SAFT-type [63,64,71,72]) has also been considered. Medeiros et al. [73] and Khan et al. [74] provided comprehensive reviews of hydrate equilibrium calculations using the van der Waals–Platteeuw theory, while the aspects of the particular theory under confinement have been discussed in [19,75].

A major requirement of the macroscopic tools developed for hydrate equilibrium calculations, in addition to their accuracy, is their computational efficiency. An accurate and computationally fast tool, at the macroscopic level, can be used for initial screening purposes in the optimization of a given separation process. Therefore, the motivation of the current study is to identify/develop such a reliable macroscopic tool that can accurately describe the hydrate equilibrium pressure of hydrates of gas mixtures, while being computationally efficient.

The objective of the current study is to perform an extensive evaluation of a simple model for three-phase equilibrium calculations of mixed gas hydrates that are of practical interest for gas-mixture separations. The model considered in this study calculates the equilibrium pressure of the mixed gas hydrate using a simple combination rule that employs (i) the hydrate dissociation pressures of the pure gases involved, and (ii) the gas mixture composition. In particular, we examine the methodology presented by Lipenkov and Istomin [76]. The particular approach has been used extensively and successfully in polar science studies [76,77], as well as research related to space science [78,79] where the temperatures are very low (i.e., below the freezing point of pure water, which is also close to the lower quadruple point, Q_1, of the corresponding hydrate systems). However, to the best of our knowledge, the particular method has not been examined systematically for cases of higher temperatures (i.e., above the Q_1), which are going to be of interest to practical industrial applications of gas-mixture separations. Gases of interest for the current study include those that are indicated in Table 1. Such gases are encountered in typical industrial applications. Some preliminary results considering some limited binary gas mixtures have been reported in an earlier study [80]. Therefore, the current work is a systematic extension of the aforementioned paper.

Table 1. Parameters for the correlation of the dissociation pressure of pure gases using Equation (3). Temperature is in K and pressure is in kPa. *T* range denotes the temperature range of applicability of the parameters. N/A denotes not applicable.

Gas	*T* Range (K)	Type of Equilibria	A_i (−)	B_i (K)	Source	Refs.
CH_4	248–273	H–I–V	14.7170	−1886.79	Holder et al. [61]	N/A
CH_4	273–298	H–L_w–V	38.9803	−8533.80	Holder et al. [61]	N/A
C_2H_6	248–273	H–I–V	17.5110	−3104.535	Holder et al. [61]	N/A
C_2H_6	273–287	H–L_w–V	44.2728	−10,424.248	Holder et al. [61]	N/A
C_2H_6	287–304	H–L_w–L_H	14.5831 ± 0.0367	−1860.741 ± 10.867	This work	[81]
C_2H_4	269–274	H–L_w–V	24.7929 ± 1.7055	−5016.239 ± 466.056	This work	[82–84]
C_2H_4	274–286	H–L_w–V	47.1247 ± 1.7384	−11,138.677 ± 490.000	This work	[83–85]
C_2H_4	286–291	H–L_w–V	42.6159 ± 0.3859	−9941.235 ± 109.283	This work	[83–85]
C_2H_4	291–295	H–L_w–L_H	120.9001 ± 2.8681	−32,679.321 ± 838.367	This work	[83,85]
C_3H_8	248–273	H–I–V	17.1560	−3269.646	Holder et al. [61]	N/A
C_3H_8	273–278	H–L_w–V	67.1301	−16,921.840	Holder et al. [61]	N/A

Table 1. *Cont.*

Gas	*T* Range (K)	Type of Equilibria	A_i (−)	B_i (K)	Source	Refs.
C_3H_8	278–303	H–L_w–L_H	14.5533 ± 0.0684	−2286.93 ± 19.215	This work	[86,87]
CO	274–285	H–L_w–V	32.4755 ± 0.1108	−8199.692 ± 31.071	This work	[88]
CO_2	248–273	H–I–V	18.5939	−3161.410	Holder et al. [61]	N/A
CO_2	273–284	H–L_w–V	44.5776	−10,245.010	Holder et al. [61]	N/A
CO_2	283–292	H–L_w–L_H	118.5425 ± 4.0947	−31,030.579 ± 1171.400	This work	[1]
N_2	248–273	H–I–V	15.1289	−1504.276	Holder et al. [61]	N/A
N_2	273–298	H–L_w–V	37.8079	−7688.626	Holder et al. [61]	N/A
H_2S	248–273	H–I–V	16.5597	−3270.409	Holder et al. [61]	N/A
H_2S	273–298	H–L_w–V	34.8278	−8266.102	Holder et al. [61]	N/A
O_2	268–271.7	H–I–V	16.7315 ± 0.0871	−2017.949 ± 23.298	This work	[89–91]
O_2	271.7–291	H–L_w–V	41.9589 ± 0.1963	−8894.429 ± 54.799	This work	[89,90,92]
SO_2	T < 270.65	H–I–V	8.9306 ±1.3650	−1579.951 ± 365.068	This work	[93–95]
SO_2	270.7–286	H–L_w–V	50.8949 ± 2.3810	−12,940.097 ± 667.712	This work	[93–95]
H_2	267–273.7	H–I–V	53.0775 ± 0.9598	−11,120.167 ± 259.541	This work	[96]
H_2	273.7–348	H–L_w–V	19.3750 ± 0.2126	−1769.473 ± 64.707	This work	[96]

The purpose of the current study is two-fold: (i) to extend the Lipenkov–Istomin methodology to mixed gas hydrate systems of industrial interest by calculating the parameters of pure components that are not available, with emphasis on conditions above the Q_1, and (ii) to evaluate the quality of the predictions of the three-phase equilibrium conditions by comparing to experimental measurements. To this purpose, reported experimental measurements (i.e., the recent experimental data collection reported by Kastanidis et al. [97] is utilized) of hydrate equilibrium pressures are compared against (i) calculations using the examined Lipenkov–Istomin methodology [76], and (ii) calculations based on a commercial simulator (CSMGem [1]). As a result, the range of applicability of the Lipenkov–Istomin method is delineated.

The remainder of the manuscript is organized as follows: Initially, the Lipenkov–Istomin methodology is briefly discussed, followed by the presentation of the extensive series of calculations for the examined hydrate-forming gas mixtures. Finally, the conclusions are presented.

2. Methodology

2.1. Calculation of Hydrate Dissociation Pressures

Lipenkov and Istomin [76] introduced a simplified methodology for calculating the hydrate dissociation pressure of a gas mixture to a first approximation, and after assuming that (i) the clathrate of the gas mixture behaves as an ideally dilute solid solution, and (ii) that the ratio of occupancies for the small and large cages is constant and the same for all guest molecules. According to the proposed methodology, the hydrate dissociation pressure of a gas mixture can be expressed as a function of the hydrate dissociation pressures of the pure gases and the corresponding mole fractions of the gas phase as follows:

$$\left(P_H^{eq}\right)_{gas-mixture} = \left(\sum_{i=1}^{n} \frac{y_i}{\left(P_H^{eq}\right)_i}\right)^{-1} \quad (1)$$

where $\left(P_H^{eq}\right)_i$ is the hydrate dissociation pressure of the pure gas i (with $i = 1, 2, \ldots, n$), and y_i is the equilibrium gas-phase mole fraction of the gas i, which belongs to a gas

mixture that contains n different components. It should be pointed out that y_i used in Equation (1) corresponds to the vapor phase that is part of the three-phase equilibrium system (i.e., Hydrate—Liquid water (or ice)—Vapor). However, a number of experimental studies, instead of reporting the measured y_i values, report the initial feed composition z_i values, which may be different compared to y_i. In the current study, we also examine the cases when z_i values are reported (i.e., y_i is replaced by z_i in Equation (1), which is a reasonable assumption) and present the corresponding results separately. Also, it should be noted that CSMGem needs the overall composition, z_i, as an input parameter and upon completion of the calculation, the resulting y_i values are very close to the corresponding z_i values. In summary, Equation (1) is a simple empirical model according to which the hydrate dissociation pressure of a gas mixture can be expressed as a function of the hydrate dissociation pressures of the pure gases and the corresponding mole fractions of the gas phase. On the other hand, CSMGem is a specifically designed model for the prediction of thermodynamically stable hydrate structures and cage occupancy. The model utilizes Gibbs energy minimization principles, providing insights into hydrate formation conditions for gas.

The hydrate dissociation pressure of the pure gas i is a function of temperature:

$$\left(P_H^{eq}\right)_i = f(T) \tag{2}$$

Within the narrow temperature ranges of interest for this study, the three-phase (H–L_w–V) equilibrium curves can be obtained rather accurately through the following simple empirical relation:

$$\ln\left(P_H^{eq}\right)_i = A^i + \frac{B_i}{T} + \frac{C_i}{T^2} + \frac{D_i}{T^3} + \dots \tag{3}$$

where A_i, B_i, C_i, D_i, etc., are component-specific parameters that are usually obtained from fitting Equation (3) to available experimental data. All of the hydrate-forming gases considered in the current study use a first-degree polynomial (with respect to $1/T$) for the description of the RHS of Equation (3), namely an Arrhenius-type description. Notice however, that a higher-degree polynomial can be used if it is deemed necessary to improve the accuracy.

2.2. Parameter Estimation

In the current study, the values for the parameters A_i and B_i are either (i) obtained from Holder et al. [61], or (ii) they are calculated in the current study using available experimental measurements. A schematic showing the steps followed in the current study is shown in Figure 1. We consider two or three different zones, depending on whether a particular hydrate-forming gas has only the lower quadruple point, Q_1 (e.g., methane), or there is also an upper quadruple point, Q_2 (e.g., propane, carbon dioxide). Therefore, for conditions below Q_1, the type of phase equilibria observed is Hydrate–Ice water–Vapor, H–I–V. For conditions above Q_1 (when no Q_2 is present) or between Q_1 and Q_2 (when Q_2 is present), the type of phase equilibria observed is Hydrate–Liquid water–Vapor, H–L_w–V. Finally, for conditions above Q_2 (when Q_2 is present), the type of phase equilibria observed is Hydrate–Liquid water–Liquid hydrocarbon/gas, H–L_w–L_H. Figure 2a is a typical example of the particular calculation for the cases of oxygen and sulfur dioxide where a first-degree polynomial is used, while Figure 2b shows the cases of carbon dioxide where a higher-degree polynomial is required for the description of the H–L_w–L_{CO2} zone.

Table 1 gives the values of the parameters A_i, and B_i, for the cases of all gases that are of interest for the current study. The parameters have been calculated by performing a regression analysis on the published experimental data (also shown in Table 1) for each pure gas hydrate, as implemented using Excel 2021. Shown also in Table 1 are the corresponding errors that resulted from the parameter estimation, as well as the temperature ranges of applicability of the empirical relation for all hydrate-forming components. The last column

of Table 1 indicates the references for the experimental data that were used in the current study for obtaining the component-specific parameters.

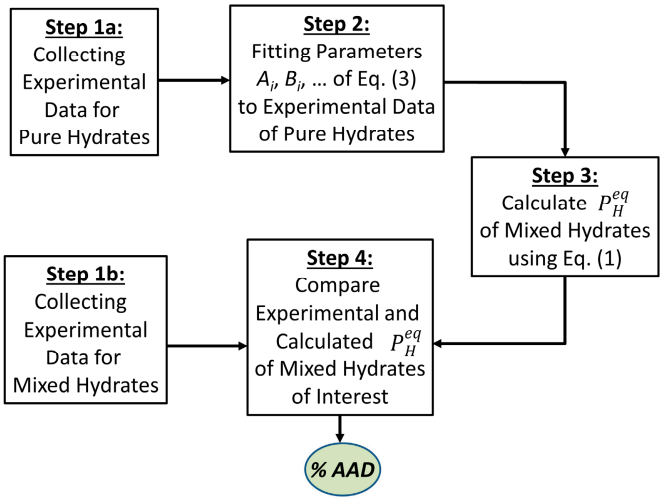

Figure 1. Schematic of the steps followed in the current study.

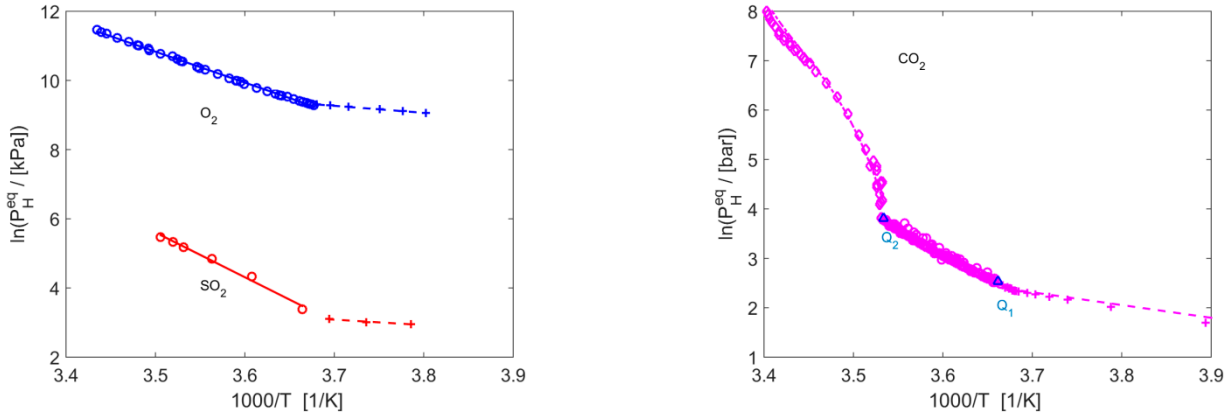

(**a**) (**b**)

Figure 2. Extended Arrhenius-type plots for the calculation of the component-specific parameters of Equation (1) for the cases of (**a**) O_2 and SO_2, and (**b**) CO_2. Experimental data are denoted with blue symbols (O_2), red symbols (SO_2), and magenta symbols (CO_2). Symbol/line code: crosses/dashed lines denote H–I–V equilibria, circles/solid lines denote H–L_w–V equilibria, and diamonds/dashed-dotted line denote H–L_w–L_H equilibria. Blue triangles indicate the lower (Q_1) and upper (Q_2) quadruple points [1] for the case of CO_2.

3. Results and Discussion

As discussed in the previous section, Lipenkov and Istomin [76] introduced a simplified methodology for calculating the hydrate dissociation pressure of a gas mixture at low temperatures (i.e., *T*s corresponding to values below the lower quadruple point, Q_1). This methodology is used in order to examine binary, ternary, and some limited quaternary mixed gas hydrates that are of industrial interest. The emphasis in the current study is on conditions above the lower quadruple point, Q_1. In this work, we use experimental data obtained from the data collection reported by Kastanidis et al. [97]. In particular, we examine the experimental hydrate systems that are indicated in Table 2. Namely, 98 publications, reporting 135 experimental mixed hydrate systems, were considered, containing a total of 2516 experimental data points.

Table 2. Hydrate-forming gas mixtures considered in the current study and the corresponding experimental studies.

Notation	System	Comment	References Examined
GM–1	CO_2 + N_2	"Flue Gas" A	[98–118]
GM–2	CO_2 + N_2 + O_2	"Flue Gas" B	[113]
GM–3	CO_2 + H_2	Methane steam reforming	[101,119–129]
GM–4	CO_2 + CH_4	Biogas upgrade	[99,103,106,108,110,112,115,117,127,130–154]
GM–5	CO_2 + gas (other)	CO_2-containing mixtures	[108,112,155–158]
GM–6	CH_4 + H_2	–	[125,148,159–163]
GM–7	CH_4 + N_2	–	[115,164–170]
GM–8	CH_4 + N_2 + O_2	"Coal-mine" gas mixture	[171]
GM–9	CH_4 + CO_2 + N_2	–	[117,148,154,166,172–179]
GM–10	CH_4 + hydrocarbon gas mixtures	CH_4-containing mixture A	[166,180–184]
GM–11	CH_4 + gas (other)	CH_4-containing mixture B	(No system considered)
GM–12	Light hydrocarbon binaries	Other cases	[166,185,186]
GM–13	H_2S + gas (other)	H_2S-containing mixtures	[128,142,187–189]
GM–14	H_2 + natural gas mixtures	H_2-containing mixtures	[128,148,160,161,190]
GM–15	Air + gas (other)	Air/N_2-containing mixtures	[91,92,191,192]

Two different comparisons are reported. In particular, we compare the hydrate dissociation pressure values that were obtained using (i) the Lipenkov–Istomin methodology (LI), and (ii) the commercial simulator CSMGem [1], against the aforementioned experimental values. The overall results of both comparisons are reported in Table 3, while additional more detailed results are reported in the Supplementary Material file. We report in Table 3 the total number of available experimental data points (*ndp*) and the percentage of the absolute average deviation in predicting the hydrate equilibrium pressure (% *AAD*) for calculations using either the equilibrium gas-phase mole fraction (y_i) or the initial feed composition (z_i), or both, depending on the information provided by each experimental study, which is calculated as follows:

$$\% \, AAD = \frac{100}{ndp} \times \sum_{i=1}^{ndp} \left| \frac{\left(P_H^{eq}\right)_i^{\exp} - \left(P_H^{eq}\right)_i^{calc}}{\left(P_H^{eq}\right)_i^{\exp}} \right| \quad (4)$$

Initially, some general conclusions are presented. For cases of hydrate-forming systems that both computational methods can be applied to, the CSMGem method performs better than the LI for gas mixtures GM–1, GM–5, GM–7, and GM–10. On the other hand, the LI approach performs better for the cases of mixtures GM–4, GM–9, GM–12, and GM–13. The better performance of the CSMGem should be expected since the parameters of the methodology are optimized in order to minimize the error in predicting the three-phase equilibrium conditions (it should also be noted that the quality of the experimental measurement affects the performance of the CSMGem approach). On the other hand, the LI is a simplified mixing rule of the equilibrium pressures of the corresponding pure components of the mixture.

Table 3. Percentage average absolute deviation (% *AAD*) during the calculation of hydrate equilibrium pressure, P_H^{eq}, for the hydrate mixture systems considered (i.e., cases of *y*-values or *z*-values reported). The number of experimental data points is denoted as *ndp*. N/A denotes that the corresponding CSMGem parameters for O_2, H_2, CO, and SO_2 are not available.

Gas Mixture System		# of Exper. Studies Examined	Total *ndp*	% *ADD* in P_H^{eq}		% *ADD* in P_H^{eq}	
				CSMGem		Lipenkov–Istomin	
				y-Values	*z*-Values	*y*-Values	*z*-Values
GM–1: $CO_2 + N_2$		20	432	15.73	25.74	7.40	17.54
GM–2: $CO_2 + N_2 + O_2$		1	4	N/A	N/A	-	14.85
GM–3: $CO_2 + H_2$		12	194	N/A	N/A	9.24	34.45
GM–4: $CO_2 + CH_4$		36	719	10.79	14.12	7.44	13.23
GM–5: CO_2 + gas (other)	$CO_2 + C_2H_6$	3	127	1.40	3.42	5.66	6.11
	$CO_2 + C_3H_8$	2	66	-	18.18	-	19.37
	$CO_2 + C_2H_6 + C_3H_8$	1	5	-	15.68	-	31.81
	$CO_2 + CO$	1	6	N/A	N/A	-	91.45
	$CO_2 + SO_2$	2	75	N/A	N/A	-	21.38
GM–6: $CH_4 + H_2$		7	338	N/A	N/A	9.38	27.61
GM–7: $CH_4 + N_2$		8	93	4.61	7.21	12.77	9.50
GM–8: $CH_4 + N_2 + O_2$		1	6	N/A	N/A	-	25.31
GM–9: $CH_4 + CO_2 + N_2$		12	146	33.77	14.11	15.79	9.66
GM–10: CH_4 + hydrocarbon gas mixtures	$CH_4 + C_2H_6$	3	35	3.15	18.72	14.38	17.30
	$CH_4 + C_3H_8$	3	38	-	13.17	-	85.03
	$CH_4 + C_2H_6 + C_3H_8$	2	20	-	6.87	-	65.16
GM–11: CH_4 + gas (other)		-	-	-	-	-	-
GM–12: Light hydrocarbon binary	$C_2H_6 + C_3H_8$	3	78	-	13.16	-	25.28
GM–13: H_2S + gas (other)	$H_2S + CO_2$	2	19	90.97	25.92	3.11	15.02
	$H_2S + CH_4$	2	11	-	8.75	-	14.58
	$H_2S + CH_4 + CO_2$	2	13	8.60	9.93	15.52	3.30
	$H_2S + CH_4 + C_3H_8$	1	10	-	128.72	-	78.83
	$H_2S + H_2 + CO_2$	1	4	N/A	N/A	24.65	48.74
GM–14: H_2 + natural gas mixtures	$H_2 + CH_4 + C_3H_8$	1	22	N/A	N/A	49.51	-
	$H_2 + CH_4 + C_2H_6 + C_3H_8$	1	16	N/A	N/A	82.69	-
	$H_2 + C_2H_4$	1	6	N/A	N/A	21.49	-
	$H_2 + CH_4 + C_2H_4$	1	4	N/A	N/A	37.33	3.73
	$H_2 + CO_2 + CH_4$	1	5	N/A	N/A	33.13	-
	$H_2 + CO_2 + H_2S$	1	4	N/A	N/A	32.41	15.42
GM–15: Air + gas (other)		4	20	N/A	N/A	-	13.90

A more detailed comparison between the two computational approaches and the experimental data is presented in the Supplementary Material file (i.e., tables included in Sections S1–S15) where a distinction is made for experimental studies published either before or after 2008. The particular year is selected since it is the year that CSMGem was made available. Therefore, experimental data that were published during earlier years could have been included (in principle) in the development of CSMGem (i.e., during

parameter optimization). On the other hand, experimental data that are published after 2008 can serve only for testing the accuracy of the considered model. In the tables included in Sections S1–S15, we report for each study the total number of available experimental data points, *ndp*, and the percentage of the absolute average deviation in predicting the hydrate equilibrium pressure, % *AAD*.

It should be noted that for gas mixtures containing either one of the gases O_2 (GM–2, GM–8, GM–15), H_2 (GM–3, GM–6, GM–13, GM–14), CO (GM–5), and SO_2 (GM–5) (also see Table 3 for particular cases considered in the current study), we report calculations in the current study only with the LI method, since optimized parameters for those components are not available in the CSMGem simulator [1].

Next, some characteristic comparison examples are plotted in Figures 3–9, and are further discussed. Figure 3 shows the comparison between experimental (denoted with circles) and calculated values with (i) the LI method (shown with solid lines), and (ii) the CSMGem simulator (shown with dashed lines), for the hydrate equilibrium pressures of the binary gas mixture: CO_2 + N_2 (GM–1). In particular, Figure 3a shows the case of the experimental data for P_H^{eq}, which are plotted as a function of y_{CO_2}, that were reported by Bruusgaard et al. [102], which were measured at constant temperature, *T*. Similarly, Figure 3b shows the case of the experimental data for P_H^{eq} plotted as a function of *T* that were reported by Olsen et al. [98], which were measured at constant feed composition, *z*. Reasonable agreement is found between the computational approaches examined (LI and CSMGem) and the two aforementioned studies.

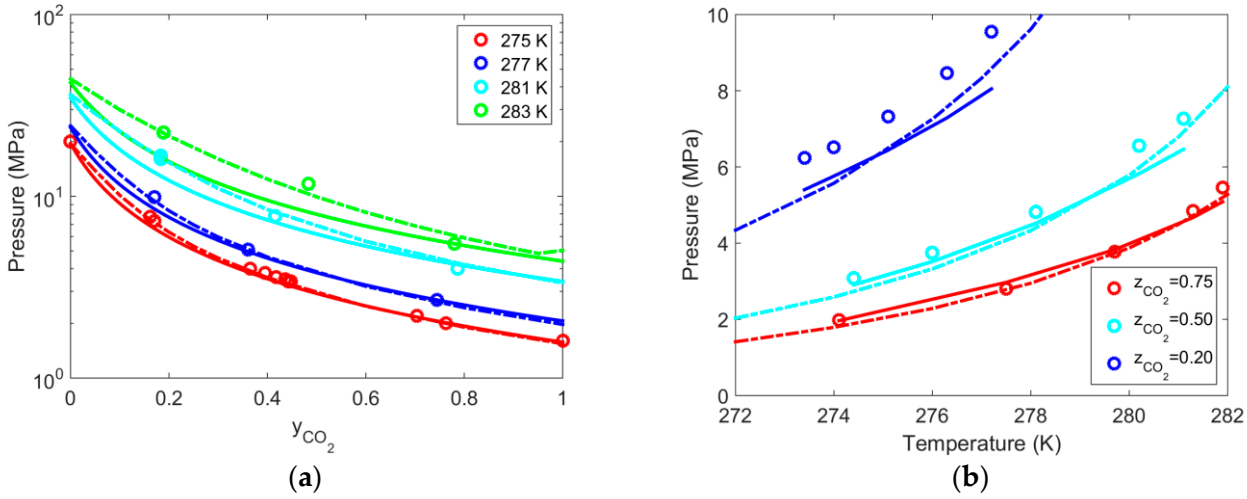

Figure 3. Comparison between experimental (denoted with circles) and calculated values (solid lines denote calculation with the current model, while dashed lines denote calculations using the CSMGem simulator [1]) for the hydrate equilibrium pressures of the binary gas mixture (GM–1): CO_2 + N_2. (**a**) Experimental data at constant *T* from Bruusgaard et al. [102], and (**b**) experimental data at constant *z* from Olsen et al. [98].

In order to further quantify the performance of the two calculation methodologies under consideration, we plotted in Figure 4 the overall % *AAD* corresponding to the calculation of the three-phase equilibrium pressure for different experimental studies for varying *T*, *y*, and *z*. Figure 4a shows the % *AAD* plotted as a function of *T*, for the experimental data of Bruusgaard et al. [102], Belandria et al. [104], and Lang et al. [105] for which studies' *y*-values have been reported. For the case of the binary gas mixture CO_2 + N_2, the CSMGem method results, in most cases, in lower % *AAD* values (i.e., less than 4%). On the other hand, for the case of the LI method, the resulting % *AAD* values vary in the range 5–30%. Furthermore, no clear/systematic trend for the % *AAD* values can be identified. For example, the % *AAD* increases when *T* increases for the experimental data of

Bruusgaard et al. [102], while the % *AAD* decreases when *T* increases for the experimental data of Belandria et al. [104].

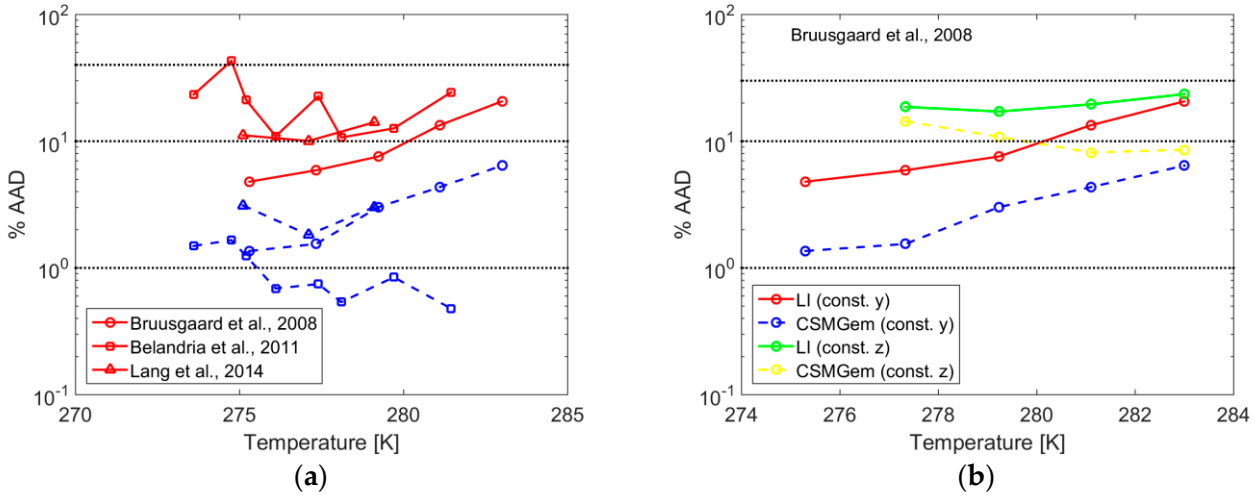

Figure 4. % *AAD* vs. *T*, resulting during the calculation of the three-phase equilibrium pressure for different experimental studies for the binary gas mixture (GM–1): CO_2 + N_2. Solid red lines denote calculations with the LI model, while dashed blue lines denote calculations using the CSMGem simulator [1]. (**a**) Experimental studies (Bruusgaard et al. [102], Belandria et al. [104], Lang and Servio [105]) reporting *y*-values, and (**b**) experimental data by Bruusgaard et al. [102]—comparison between experimental measurements reporting *y*- or *z*-values.

The corresponding figures for % *AAD* plotted as a function of y_{CO_2} (Figure S1a) or z_{CO_2} (Figure S1b) are shown in Figure S1 of the Supplementary Material. For most cases shown, the % *AAD* values are lower than 20% for the case of the CSMGem method, while on the other hand, they are lower than 40% for the case of the LI method. It should be noted that for the case of the experimental data of Herri et al. [103], the LI method results in lower % *AAD* values when compared to CSMGem values, which is a notable exception for the gas mixture GM–1. Additional exceptions include the experimental data of Belandria et al. [104] and Le Quang et al. [106].

Figure 4b utilizes the experimental data reported by Bruusgaard et al. [102] in order to assess the effect of using the available initial feed composition z_i values in Equation (1), instead of the required measured y_i values. For the particular experimental data set, it is clear that for both methods (i.e., LI and CSMGem) we obtain lower values for % *AAD* when y_i values are used. The difference in % *AAD* is higher at lower *T*s. As *T* increases and the upper quadruple point, Q_2, for CO_2 is approached (i.e., *T* = 283.0 K), we observe that the % *AAD* for the cases of y_i or z_i values is converging asymptotically. A more detailed discussion on Q_2 for the case of CO_2 can be found in Kastanidis et al.'s report [193]. In addition, from Table 3, we can observe that for the vast majority of cases, the % *AAD* values when y_i values are reported are lower than those when z_i values are reported.

Similarly, Figure 5 shows the comparison between experimental and calculated values for the hydrate equilibrium pressures of the binary gas mixture: CO_2 + CH_4 (GM–4). In particular, Figure 5a shows the case of the experimental data of Belandria et al. [138], which were measured at constant temperature, *T*, while Figure 5b shows the case of the experimental data of Seo et al. [135], which were measured at constant pressure, *P*. For both cases, experimental values for y_i have been reported.

A general observation that can be made from the figures shown, as well as from all the calculations that were performed, is that the % *AAD* in hydrate equilibrium predictions increases as the hydrate equilibrium pressure (or temperature) increases. For hydrate equilibrium pressures that are below 10 MPa, the % *AAD* is kept well below 8–10%. Therefore, the accuracy of the methodology deteriorates as we go with higher pressures.

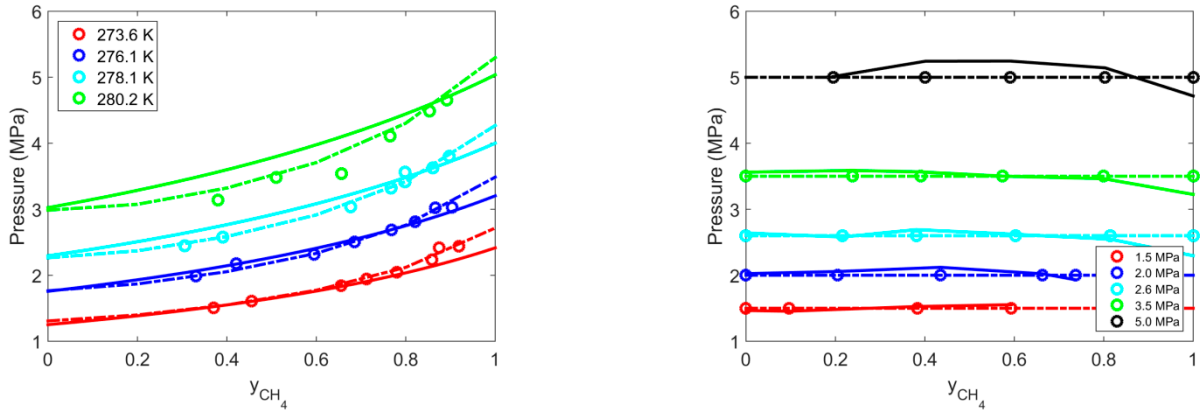

Figure 5. Comparison between experimental (denoted with circles) and calculated values (solid lines denote calculation of the current study, while dashed lines denote calculations using the CSMGem simulator [1]) for the hydrate equilibrium pressures of the binary gas mixture (GM–4): CH_4 + CO_2. (**a**) Experimental data at constant T from Belandria et al. [138], and (**b**) experimental data at constant P from Seo et al. [135].

We can further observe in Table 3 that for the case of gas mixture GM–4, the LI method gives lower overall % *AAD* values. Some typical examples are also shown in Figure 6, where we plot the % *AAD* as a function of T for several experimental studies, which provide y-values (Figure 6a) or z-values (Figure 6b). Additional plots showing the % *AAD* as a function of y_{CH_4} (Figure S2a) or z_{CH_4} (Figure S2b,c) are shown in Figure S2 of the Supplementary Material. It is evident that for most cases of experimental data sets (e.g., Adisasmito et al. [131] (e.g., see Figure S2a), Unruh et al. [130], Servio et al. [194], Lee et al. [146], Belandria et al. [138,145], Sfaxi et al. [110], Sadeq et al. [115] (e.g., see Figure S2b,c)), the % *AAD* values are lower than 10%, or in the range 10–20% (e.g., Beltran et al. [136], Bruusgaard et al. [137], Belandria et al. [138] (e.g., see Figure 6a,b)). Only a few exceptions to the aforementioned rule have been identified. Namely, the experimental data of Obanijesu et al. [148] and Legoix et al. [117,151] have % *AAD* values in the range 30–60% (see Figure S2b and Tables in Section S4 of the Supplementary Material). Given that the calculations (LI or CSMGem) for the other experimental data sets result in % *AAD*s with significantly lower values, this could lead to the conclusion that the three particular data sets may have problematic experimental measurements that could be resolved by performing additional experimental measurements under similar conditions.

Figure 7 examines the case of the binary gas hydrate CH_4 + N_2 (GM–7). It shows the case of the experimental data for P_H^{eq} plotted as a function of T, measured at constant feed composition, z. In particular, Figure 7a,b show the experimental data of Sadeq et al. [115], while Figure 7c,d show the experimental data of Lee et al. [167]. As can be seen from Figure 7 and also Table S7 of the Supplementary Material for the particular experimental data sets, both methods considered in the current study give similar results. Overall, for the case of gas mixture GM–7, CSMGem performs slightly better than the LI method. In particular, CSMGem has a % *AAD* equal to 4.48% with the corresponding LI equal to 12.57% for cases when y is reported. On the other hand, CSMGem has a % *AAD* equal to 9.50% with the corresponding LI equal to 7.20% for cases when z is reported. Additional comparisons are provided in Figure S3 of the Supplementary Material, where the % *AAD* values are plotted as a function of z_{CH_4}. The majority of cases result in % *AAD* values that are less than 10%, while a limited number of cases are in the range 10–20%.

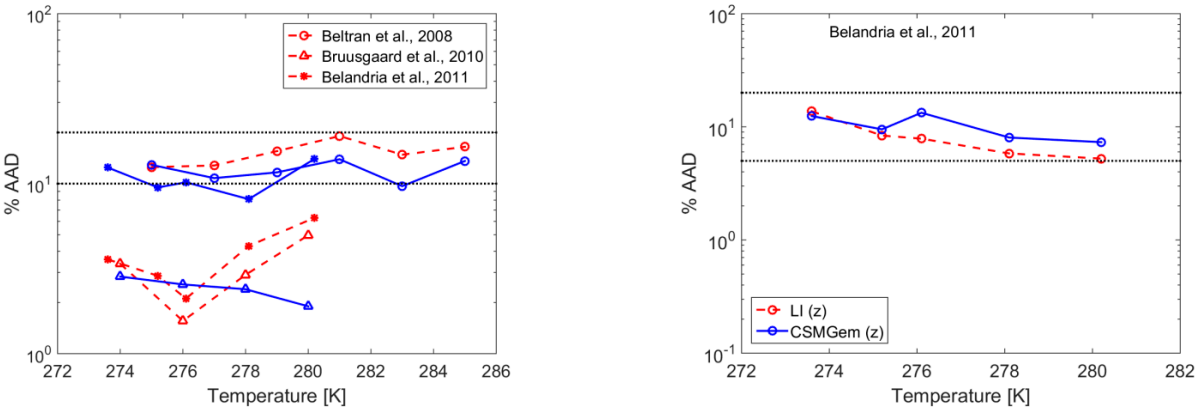

(**a**) (**b**)

Figure 6. % *AAD* vs. *T*, resulting during the calculation of the three-phase equilibrium pressure for different experimental studies for the binary gas mixture (GM–4): CH_4 + CO_2. Dashed redlines denote calculation of the current study (LI), while solid blue lines denote calculations using the CSMGem simulator [1]. (**a**) Experimental studies (Beltran et al. [136], Bruusgaard et al. [137], Belandria et al. [138]) reporting *y*-values, and (**b**) experimental data by Belandria et al. [138] reporting *z*-values.

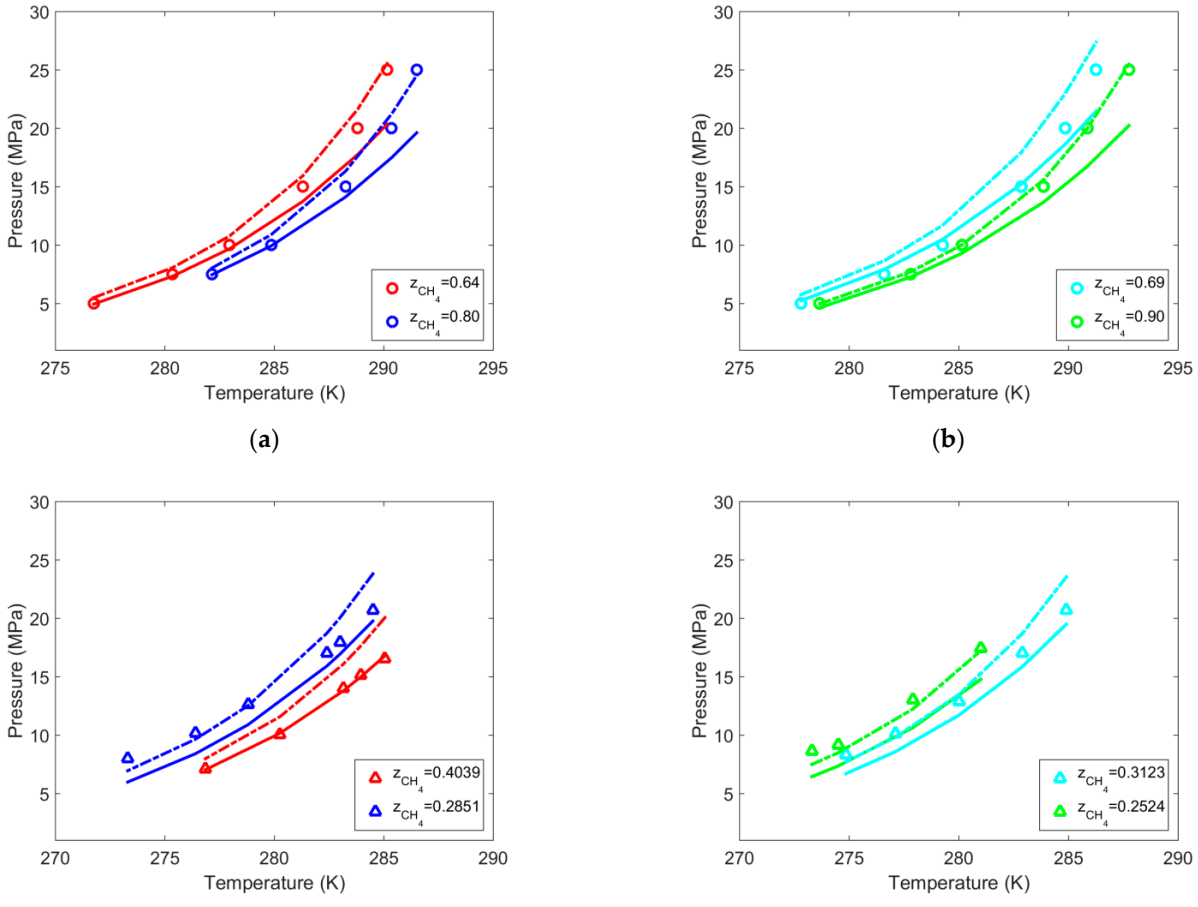

(**a**) (**b**)

(**c**) (**d**)

Figure 7. Comparison between experimental (denoted with circles) and calculated values (solid lines denote calculation of the current study, while dashed lines denote calculations using the CSMGem simulator [1]) for the hydrate equilibrium pressures of the binary gas mixture (GM–7): CH_4 + N_2. (**a**,**b**) Experimental data at constant *z* from Sadeq et al. [77]. (**c**,**d**) Experimental data at constant z from Lee et al. [83].

Figure 8 shows the comparison between experimental and calculated (LI method) values for the hydrate equilibrium pressures of the binary gas mixture CO_2 + H_2 (GM–3). In particular, Figure 8a shows the case of the experimental data for P_H^{eq} as a function of y_{CO_2} that were reported by Sugahara et al. [119], which were measured at constant temperature, T. Similarly, Figure 8b shows the case of the experimental data for P_H^{eq} as a function of T that were reported by Kumar et al. [120], which were measured at constant feed composition, z.

Figure S4 of the Supplementary Material shows additional comparisons for the gas mixture GM–3. Namely, Figure S4a shows the % *AAD* values for the prediction of the three-phase equilibrium pressure of three experimental studies (Sugahara et al. [119], Belandria et al. [121] (reporting y-values), and Belandria et al. [121] (reporting z-values)) plotted as a function of T. Figure S4b shows the corresponding % *AAD* values of all available experimental data (Table S3 of the Supplementary Material) plotted as a function of z_{CO_2}. The majority of the cases result in % *AAD* values in the range 10–50%, while for the case of Belandria et al. (y-values), the % *AAD* values are lower than 8%.

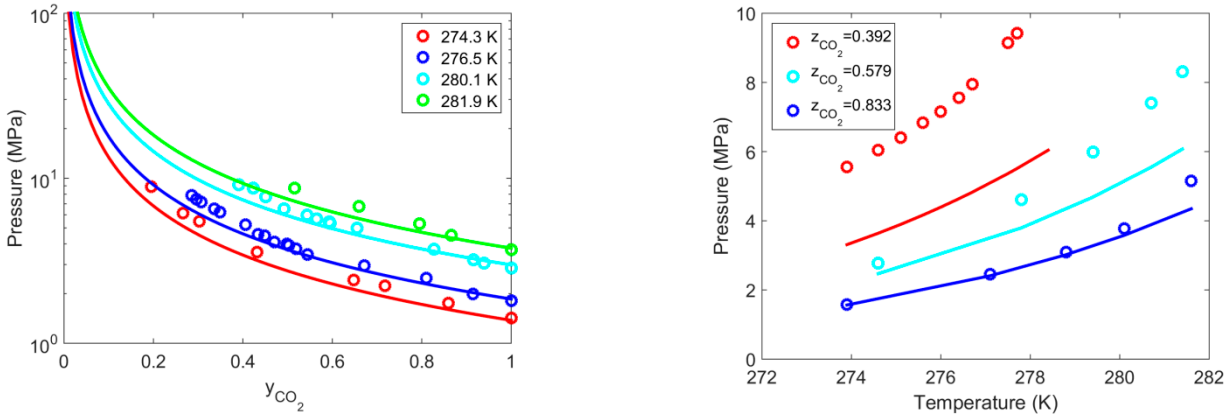

(**a**) (**b**)

Figure 8. Comparison between experimental (denoted with circles) and calculated values with the LI methodology (denoted with solid lines) for the hydrate equilibrium pressures of the binary gas mixture (GM–3): CO_2 + H_2. (**a**) Experimental data at constant T from Sugahara et al. [119], and (**b**) experimental data at constant z from Kumar et al. [120].

Figure 9 shows the comparison between experimental and calculated (LI method) values for the hydrate equilibrium pressures of the binary gas mixture CH_4 + H_2 (GM–6). Figure 9a shows the case of the experimental data for P_H^{eq} as a function of T that were reported by Pang et al. [125], which were measured at constant feed composition, z, while Figure 9b shows the corresponding cases of the experimental data of Zhang et al. [161], and Obanijesu et al. [148].

Additional comparisons are provided in Figure S5 of the Supplementary Material, where the % *AAD* values for the prediction of the three-phase equilibrium pressure of four experimental studies (Zhang et al. [161], Skiba et al. [162], Pang et al. [125], and Obanijesu et al. [148]) are plotted as a function of z_{CH_4}. The majority of cases result in % *AAD* values that are less than 10%, while a limited number of cases have % *AAD* values that are in the range 10–20%.

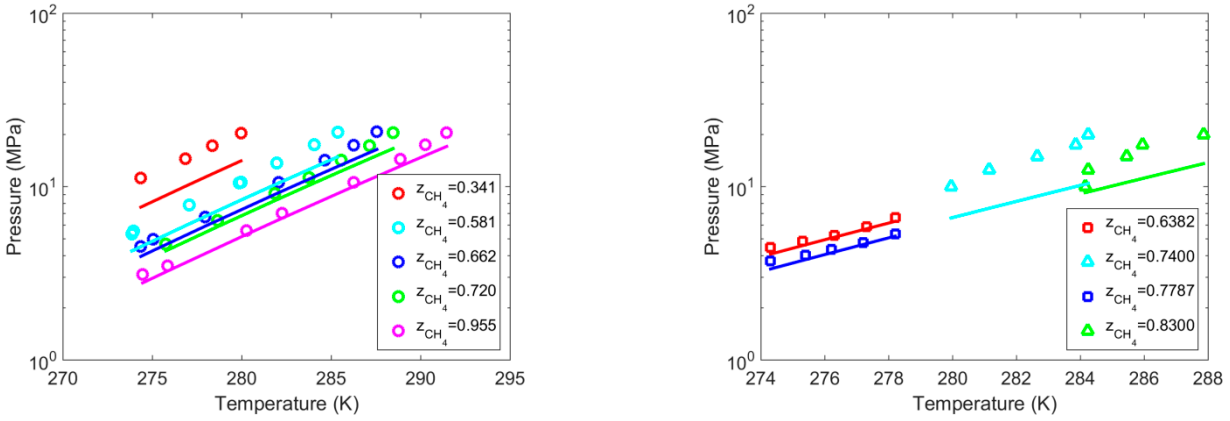

Figure 9. Comparison between experimental (denoted with symbols) and calculated values with the LI methodology (denoted with solid lines) for the hydrate equilibrium pressures of the binary gas mixture (GM–6): CH_4 + H_2. (**a**) Experimental data at constant *T* from Pang et al. [125] (denoted with circles), and (**b**) experimental data at constant *T* from Zhang et al. [161] (denoted with squares) and Obanijesu et al. [148] (denoted with triangles).

4. Model Limitations

Macroscopic tools developed for hydrate equilibrium calculations need to be (i) accurate, and (ii) computationally efficient. An accurate and computationally fast tool can be used for initial screening purposes in the optimization of a given separation process. The identification/development of such a reliable macroscopic tool that can accurately describe the hydrate equilibrium pressure of hydrates of gas mixtures, while being computationally efficient, is the main motivation of the current study. The current section summarizes the limitations of the examined/proposed LI methodology.

(1) In the current study, the vast majority of the experimental data that were examined have *P* and *T* conditions that are between the upper and lower quadruple points of the participating pure components in the hydrate-forming gas mixtures. From the analysis in this work, we can conclude that the presence of a component exhibiting an upper quadruple point, Q_2, results in calculations of the hydrate equilibrium pressures with the LI method that have usually higher values of % *AAD*, particularly at the proximity or above Q_2. Therefore, it would be of interest to conduct a more systematic study of such hydrate systems (i.e., containing CO_2, H_2S, C_2H_4, C_3H_6, etc.), particularly at the proximity or above Q_2. Such aspects, however, which may also include structural transition phenomena (i.e., sII to sI), are beyond the scope of the current study and are left for the future.

(2) The examined LI methodology is not capable of providing any information regarding cage occupancies. For the case of methods that couple the van der Waals–Platteeuw statistical theory with an EoS, such as the CSMGem method, the calculation of cage occupancies is a side result obtained during the calculation of three-phase equilibrium conditions.

(3) The LI methodology is applicable to mixtures with components for which the parameters A_i and B_i, for calculating the equilibrium pressure (via Equation (3)) of the pure component, are available. Namely, the methodology is limited to hydrate-forming components listed in Table 1. Therefore, in order to extend the methodology to other components, an approach such as the one described in the flowchart, shown in Figure 1, should be followed.

5. Conclusions

In this work, we have considered a simple methodology, called LI, for the calculation of the hydrate equilibrium pressure of gas mixtures. Gas mixtures of interest for this study were binary, ternary, and limited quaternary mixtures that were made up of different combinations of eleven components (i.e., CH_4, C_2H_6, C_2H_4, C_3H_8, CO, CO_2, N_2, H_2S, O_2,

SO_2, and H_2). In total, 98 publications, reporting 135 experimental mixed hydrate systems, were considered, containing a total of 2516 experimental data points. Such gas mixtures are encountered in practical industrial applications of gas-mixture separations.

An extensive series of calculations using the examined LI methodology were performed and the calculations were compared against available experimental measurements, as well as with the CSMGem simulator. It should be noted that the intent of the study is not to replace the CSMGem simulator with the proposed methodology but to examine if a simpler and more computationally efficient approach can produce reasonable results (at least within some specific temperature, pressure, and composition range) that can be used during the preliminary stage of the design of processes. After all, the theoretical basis behind CSMGem or other similar van der Waals–Platteeuw-based models is significantly stronger than the simplified LI approach.

Reasonable agreement between experiments and calculations with the LI methodology was obtained, considering its simplicity. The agreement was found to be better at lower hydrate equilibrium pressures.

Finally, higher deviations have been observed for hydrate-forming gas mixtures that contain a component exhibiting an upper quadruple point, Q_2, particularly at the proximity of Q_2. Such systems require a more detailed study in order to examine if the performance of the LI method can be further improved. This aspect is left for a future study.

Supplementary Materials: The following are available online at: https://www.mdpi.com/article/10.3390/en17020440/s1, Sections S1–S15 contain a detailed presentation of the calculations with the LI approach and the CSMGem simulator. Figures S1–S5 show additional plots of % *AAD* vs. *T*, *y*, or *z*.

Author Contributions: Conceptualization, I.N.T.; methodology, I.N.T. and P.K.; software, P.K. and I.N.T.; validation, P.K. and I.N.T.; formal analysis, P.K. and I.N.T.; writing—original draft preparation, I.N.T. and P.K.; writing—review and editing, I.N.T., P.K., G.E.R., G.P., E.V. and A.K.S.; supervision, I.N.T., G.E.R., E.V. and A.K.S.; project administration, I.N.T.; funding acquisition, A.K.S. All authors have read and agreed to the published version of the manuscript.

Funding: A.K.S. acknowledges partial support by the project "NCSRD—INRASTES research activities in the framework of the national RIS3" (MIS 5002559), which is implemented under the "Action for the Strategic Development on the Research and Technological Sector", funded by the Operational Programme "Competitiveness, Entrepreneurship and Innovation" (NSRF 2014–2020) and co-financed by Greece and the European Union (European Regional Development Fund).

Data Availability Statement: Data is contained within the article (and Supplementary Materials).

Conflicts of Interest: The authors declare no conflicts of interest.

Nomenclature

$\%AAD$	% absolute average deviation, defined by Equation (4)
A_i	Component-specific parameter of Equation (3)
B_i	Component-specific parameter of Equation (3)
C_i	Component-specific parameter of Equation (3)
D_i	Component-specific parameter of Equation (3)
f	Symbol denoting a function
n	Number of components in the gas mixture
ndp	Number of experimental data points
P_H^{eq}	Hydrate equilibrium pressure (Pa)
T	Temperature (K)
T_{eq}	Hydrate equilibrium temperature (K)
y	Gas composition expressed as mole fraction (–)
z	Initial feed composition expressed as mole fraction (–)
Subscripts:	
i	Component i of a mixture with n gas components
gas-mixture	Denotes property of the gas mixture
H	Hydrate

Superscripts:

calc	Calculated
eq	Equilibrium
exp	Experimental

References

1. Dendy Sloan, E.; Koh, C. *Clathrate Hydrates of Natural Gases*, 3rd ed.; Taylor & Francis, Ed.; Chemical Industries; CRC Press: Boca Raton, FL, USA, 2007; Volume 20074156, ISBN 978-0-8493-9078-4.
2. Sloan, E.D. Fundamental Principles and Applications of Natural Gas Hydrates. *Nature* **2003**, *426*, 353. [CrossRef] [PubMed]
3. Koh, C.A. Towards a Fundamental Understanding of Natural Gas Hydrates. *Chem. Soc. Rev.* **2002**, *31*, 157–167. [CrossRef] [PubMed]
4. Walsh, M.R.; Hancock, S.H.; Wilson, S.J.; Patil, S.L.; Moridis, G.J.; Boswell, R.; Collett, T.S.; Koh, C.A.; Sloan, E.D. Preliminary Report on the Commercial Viability of Gas Production from Natural Gas Hydrates. *Energy Econ.* **2009**, *31*, 815–823. [CrossRef]
5. Moridis, G.J.; Collett, T.S.; Boswell, R.; Kurihara, M.; Reagan, M.T.; Koh, C.; Sloan, E.D. Toward Production From Gas Hydrates: Current Status, Assessment of Resources, and Simulation-Based Evaluation of Technology and Potential. *SPE Reserv. Eval. Eng.* **2009**, *12*, 745–771. [CrossRef]
6. Collett, T.; Bahk, J.J.; Baker, R.; Boswell, R.; Divins, D.; Frye, M.; Goldberg, D.; Husebø, J.; Koh, C.; Malone, M.; et al. Methane Hydrates in Nature-Current Knowledge and Challenges. *J. Chem. Eng. Data* **2015**, *60*, 319–329. [CrossRef]
7. Chong, Z.R.; Yang, S.H.B.; Babu, P.; Linga, P.; Li, X.S. Review of Natural Gas Hydrates as an Energy Resource: Prospects and Challenges. *Appl. Energy* **2016**, *162*, 1633–1652. [CrossRef]
8. Tsimpanogiannis, I.N.; Costandy, J.; Kastanidis, P.; El Meragawi, S.; Michalis, V.K.; Papadimitriou, N.I.; Karozis, S.N.; Diamantonis, N.I.; Moultos, O.A.; Romanos, G.E.; et al. Using Clathrate Hydrates for Gas Storage and Gas-Mixture Separations: Experimental and Computational Studies at Multiple Length Scales. *Mol. Phys.* **2018**, *116*, 2041–2060. [CrossRef]
9. Kennett, J.P.; Cannariato, K.G.; Hendy, I.L.; Behl, R.J. *Methane Hydrates in Quaternary Climate Change: The Clathrate Gun Hypothesis*; American Geophysical Union: Washington, DC, USA, 2003; ISBN 0-87590-296-0.
10. Ruppel, C.D.; Kessler, J.D. The Interaction of Climate Change and Methane Hydrates. *Rev. Geophys.* **2017**, *55*, 126–168. [CrossRef]
11. Kelland, M.A. History of the Development of Low Dosage Hydrate Inhibitors. *Energy Fuels* **2006**, *20*, 825–847. [CrossRef]
12. Zerpa, L.E.; Salager, J.-L.; Koh, C.A.; Sloan, E.D.; Sum, A.K. Surface Chemistry and Gas Hydrates in Flow Assurance. *Ind. Eng. Chem. Res.* **2011**, *50*, 188–197. [CrossRef]
13. Kelland, M.A. A Review of Kinetic Hydrate Inhibitors from an Environmental Perspective. *Energy Fuels* **2018**, *32*, 12001–12012. [CrossRef]
14. Vanneste, M.; Sultan, N.; Garziglia, S.; Forsberg, C.F.; L'Heureux, J.-S. Seafloor Instabilities and Sediment Deformation Processes: The Need for Integrated, Multi-Disciplinary Investigations. *Mar. Geol.* **2014**, *352*, 183–214. [CrossRef]
15. McConnell, D.R.; Zhang, Z.; Boswell, R. Review of Progress in Evaluating Gas Hydrate Drilling Hazards. *Mar. Pet. Geol.* **2012**, *34*, 209–223. [CrossRef]
16. Milkov, A.V. Global Estimates of Hydrate-Bound Gas in Marine Sediments: How Much Is Really Out There? *Earth Sci. Rev.* **2004**, *66*, 183–197. [CrossRef]
17. Klauda, J.B.; Sandler, S.I. Global Distribution of Methane Hydrate in Ocean Sediment. *Energy Fuels* **2005**, *19*, 459–470. [CrossRef]
18. Piñero, E.; Marquardt, M.; Hensen, C.; Haeckel, M.; Wallmann, K. Estimation of the Global Inventory of Methane Hydrates in Marine Sediments Using Transfer Functions. *Biogeosciences* **2013**, *10*, 959–975. [CrossRef]
19. Li, X.S.; Zhang, Y.; Li, G.; Chen, Z.Y.; Yan, K.F.; Li, Q.P. Gas Hydrate Equilibrium Dissociation Conditions in Porous Media Using Two Thermodynamic Approaches. *J. Chem. Thermodyn.* **2008**, *40*, 1464–1474. [CrossRef]
20. Yang, L.; Shi, K.; Qu, A.; Liang, H.; Li, Q.; Lv, X.; Leng, S.; Liu, Y.; Zhang, L.; Liu, Y.; et al. The Locally Varying Thermodynamic Driving Force Dominates the Gas Production Efficiency from Natural Gas Hydrate-Bearing Marine Sediments. *Energy* **2023**, *276*, 127545. [CrossRef]
21. Waite, W.F.; Santamarina, J.C.; Cortes, D.D.; Dugan, B.; Espinoza, D.N.; Germaine, J.; Jang, J.; Jung, J.W.; Kneafsey, T.J.; Shin, H.; et al. Physical Properties of Hydrate-Bearing Sediments. *Rev. Geophys.* **2009**, *47*, RG4003. [CrossRef]
22. Tsimpanogiannis, I.N. Study of the Critical Gas Saturation during Methane Hydrate Dissociation at the Single-Pore Scale: Analytical Solutions for Large Pores. *J. Nat. Gas Sci. Eng.* **2020**, *83*, 103577. [CrossRef]
23. Tsimpanogiannis, I.N.; Stamatakis, E.; Stubos, A.K. Study of the Critical Pore Radius That Results in Critical Gas Saturation during Methane Hydrate Dissociation at the Single-Pore Scale: Analytical Solutions for Small Pores and Potential Implications to Methane Production from Geological Media. *Energies* **2022**, *15*, 210. [CrossRef]
24. Li, X.S.; Xu, C.G.; Zhang, Y.; Ruan, X.K.; Li, G.; Wang, Y. Investigation into Gas Production from Natural Gas Hydrate: A Review. *Appl. Energy* **2016**, *172*, 286–322. [CrossRef]
25. Khokhar, A.A.; Gudmundsson, J.S.; Sloan, E.D. Gas Storage in Structure H Hydrates. *Fluid Phase Equilib.* **1998**, *150–151*, 383–392. [CrossRef]
26. Susilo, R.; Alavi, S.; Ripmeester, J.; Englezos, P. Tuning Methane Content in Gas Hydrates via Thermodynamic Modeling and Molecular Dynamics Simulation. *Fluid Phase Equilib.* **2008**, *263*, 6–17. [CrossRef]

27. Mao, W.L.; Mao, H.-K.K.; Goncharov, A.F.; Struzhkin, V.V.; Guo, Q.; Hu, J.; Shu, J.; Hemley, R.J.; Somayazulu, M.; Zhao, Y. Hydrogen Clusters in Clathrate Hydrate. *Science* **2002**, *297*, 2247–2249. [CrossRef]
28. Veluswamy, H.P.; Kumar, R.; Linga, P. Hydrogen Storage in Clathrate Hydrates: Current State of the Art and Future Directions. *Appl. Energy* **2014**, *122*, 112–132. [CrossRef]
29. Tsimpanogiannis, I.N.; Economou, I.G.; Stubos, A.K. A Practical Methodology to Estimate the H_2 Storage Capacity of Pure and Binary Hydrates Based on Monte Carlo Simulations. *J. Chem. Eng. Data* **2020**, *65*, 1289–1299. [CrossRef]
30. Kang, S.-P.; Lee, H. Recovery of CO_2 from Flue Gas Using Gas Hydrate: Thermodynamic Verification through Phase Equilibrium Measurements. *Environ. Sci. Technol.* **2000**, *34*, 4397–4400. [CrossRef]
31. Seo, Y.-T.; Moudrakovski, I.L.; Ripmeester, J.A.; Lee, J.; Lee, H. Efficient Recovery of CO_2 from Flue Gas by Clathrate Hydrate Formation in Porous Silica Gels. *Environ. Sci. Technol.* **2005**, *39*, 2315–2319. [CrossRef]
32. Dabrowski, N.; Windmeier, C.; Oellrich, L.R. Purification of Natural Gases with High CO_2 Content Using Gas Hydrates. *Energy Fuels* **2009**, *23*, 5603–5610. [CrossRef]
33. Adeyemo, A.; Kumar, R.; Linga, P.; Ripmeester, J.; Englezos, P. Capture of Carbon Dioxide from Flue or Fuel Gas Mixtures by Clathrate Crystallization in a Silica Gel Column. *Int. J. Greenh. Gas Control.* **2010**, *4*, 478–485. [CrossRef]
34. Babu, P.; Kumar, R.; Linga, P. Unusual Behavior of Propane as a Co-Guest during Hydrate Formation in Silica Sand: Potential Application to Seawater Desalination and Carbon Dioxide Capture. *Chem. Eng. Sci.* **2014**, *117*, 342–351. [CrossRef]
35. Babu, P.; Nambiar, A.; He, T.; Karimi, I.A.; Lee, J.D.; Englezos, P.; Linga, P. A Review of Clathrate Hydrate Based Desalination to Strengthen Energy-Water Nexus. *ACS Sustain. Chem. Eng.* **2018**, *6*, 8093–8107. [CrossRef]
36. Tsimpanogiannis, I.N.; Jamali, S.H.; Economou, I.G.; Vlugt, T.J.H.; Moultos, O.A. On the Validity of the Stokes–Einstein Relation for Various Water Force Fields. *Mol. Phys.* **2020**, *118*, e1702729. [CrossRef]
37. Tsimpanogiannis, I.N.; Maity, S.; Celebi, A.T.; Moultos, O.A. Engineering Model for Predicting the Intradiffusion Coefficients of Hydrogen and Oxygen in Vapor, Liquid, and Supercritical Water Based on Molecular Dynamics Simulations. *J. Chem. Eng. Data* **2021**, *66*, 3226–3244. [CrossRef]
38. Vatamanu, J.; Kusalik, P.G. Molecular Insights into the Heterogeneous Crystal Growth of SI Methane Hydrate. *J. Phys. Chem. B* **2006**, *110*, 15896–15904. [CrossRef] [PubMed]
39. English, N.J.; Phelan, G.M. Molecular Dynamics Study of Thermal-Driven Methane Hydrate Dissociation. *J. Chem. Phys.* **2009**, *131*, 074704. [CrossRef]
40. Alavi, S.; Ripmeester, J.A. Nonequilibrium Adiabatic Molecular Dynamics Simulations of Methane Clathrate Hydrate Decomposition. *J. Chem. Phys.* **2010**, *132*, 144703. [CrossRef]
41. Conde, M.M.; Vega, C. Determining the Three-Phase Coexistence Line in Methane Hydrates Using Computer Simulations. *J. Chem. Phys.* **2010**, *133*, 064507. [CrossRef]
42. Jacobson, L.C.; Molinero, V. Can Amorphous Nuclei Grow Crystalline Clathrates? The Size and Crystallinity of Critical Clathrate Nuclei. *J. Am. Chem. Soc.* **2011**, *133*, 6458–6463. [CrossRef]
43. Michalis, V.K.; Costandy, J.; Tsimpanogiannis, I.N.; Stubos, A.K.; Economou, I.G. Prediction of the Phase Equilibria of Methane Hydrates Using the Direct Phase Coexistence Methodology. *J. Chem. Phys.* **2015**, *142*, 044501. [CrossRef] [PubMed]
44. Costandy, J.; Michalis, V.K.; Tsimpanogiannis, I.N.; Stubos, A.K.; Economou, I.G. The Role of Intermolecular Interactions in the Prediction of the Phase Equilibria of Carbon Dioxide Hydrates. *J. Chem. Phys.* **2015**, *143*, 094506. [CrossRef] [PubMed]
45. Michalis, V.K.; Tsimpanogiannis, I.N.; Stubos, A.K.; Economou, I.G. Direct Phase Coexistence Molecular Dynamics Study of the Phase Equilibria of the Ternary Methane–Carbon Dioxide–Water Hydrate System. *Phys. Chem. Chem. Phys.* **2016**, *18*, 23538–23548. [CrossRef] [PubMed]
46. Tsimpanogiannis, I.N.; Michalis, V.K.; Economou, I.G. Enthalpy of Dissociation of Methane Hydrates at a Wide Pressure and Temperature Range. *Fluid Phase Equilib.* **2019**, *489*, 30–40. [CrossRef]
47. Finney, A.R.; Rodger, P.M. Applying the Z Method to Estimate Temperatures of Melting in Structure II Clathrate Hydrates. *Phys. Chem. Chem. Phys.* **2011**, *13*, 19979. [CrossRef]
48. Wierzchowski, S.J.; Monson, P.A. Calculation of Free Energies and Chemical Potentials for Gas Hydrates Using Monte Carlo Simulations. *J. Phys. Chem. B* **2007**, *111*, 7274–7282. [CrossRef]
49. Sizov, V.V.; Piotrovskaya, E.M. Computer Simulation of Methane Hydrate Cage Occupancy. *J. Phys. Chem. B* **2007**, *111*, 2886–2890. [CrossRef]
50. Papadimitriou, N.I.; Tsimpanogiannis, I.N.; Papaioannou, A.T.; Stubos, A.K. Evaluation of the Hydrogen-Storage Capacity of Pure H_2 and Binary H_2-THF Hydrates with Monte Carlo Simulations. *J. Phys. Chem. C* **2008**, *112*, 10294–10302. [CrossRef]
51. Papadimitriou, N.I.; Tsimpanogiannis, I.N.; Stubos, A.K.; Martin, A.; Rovetto, L.J.; Peters, C.J. Unexpected Behavior of Helium as Guest Gas in SII Binary Hydrates. *J. Phys. Chem. Lett.* **2010**, *1*, 1014–1017. [CrossRef]
52. Jensen, L.; Thomsen, K.; von Solms, N.; Wierzchowski, S.; Walsh, M.R.; Koh, C.A.; Sloan, E.D.; Wu, D.T.; Sum, A.K. Calculation of Liquid Water−Hydrate−Methane Vapor Phase Equilibria from Molecular Simulations. *J. Phys. Chem. B* **2010**, *114*, 5775–5782. [CrossRef]
53. Papadimitriou, N.I.; Tsimpanogiannis, I.N.; Stubos, A.K.; Martín, A.; Rovetto, L.J.; Florusse, L.J.; Peters, C.J. Experimental and Computational Investigation of the SII Binary He−THF Hydrate. *J. Phys. Chem. B* **2011**, *115*, 1411–1415. [CrossRef] [PubMed]
54. Papadimitriou, N.I.; Tsimpanogiannis, I.N.; Economou, I.G.; Stubos, A.K. Storage of Methane in Clathrate Hydrates: Monte Carlo Simulations of SI Hydrates and Comparison with Experimental Measurements. *J. Chem. Eng. Data* **2016**, *61*, 2886–2896. [CrossRef]

55. Brumby, P.E.; Yuhara, D.; Wu, D.T.; Sum, A.K.; Yasuoka, K. Cage Occupancy of Methane Hydrates from Gibbs Ensemble Monte Carlo Simulations. *Fluid Phase Equilib.* **2016**, *413*, 242–248. [CrossRef]
56. Papadimitriou, N.I.; Tsimpanogiannis, I.N.; Economou, I.G.; Stubos, A.K. Influence of Combining Rules on the Cavity Occupancy of Clathrate Hydrates by Monte Carlo Simulations. *Mol. Phys.* **2014**, *112*, 2258–2274. [CrossRef]
57. Tsimpanogiannis, I.N.; Economou, I.G. Monte Carlo Simulation Studies of Clathrate Hydrates: A Review. *J. Supercrit. Fluids* **2018**, *134*, 51–60. [CrossRef]
58. van der Waals, J.H.; Platteeuw, J.C. Clathrate Solutions. *Adv. Chem. Phys.* **1959**, *2*, 1–57.
59. Parrish, W.R.; Prausnitz, J.M. Dissociation Pressures of Gas Hydrates Formed by Gas Mixtures. *Ind. Eng. Chem. Process Des. Dev.* **1972**, *11*, 26–35. [CrossRef]
60. Holder, G.D.; Corbin, G.; Papadopoulos, K.D. Thermodynamic and Molecular Properties of Gas Hydrates from Mixtures Containing Methane, Argon, and Krypton. *Ind. Eng. Chem. Fundam.* **1980**, *19*, 282–286. [CrossRef]
61. Holder, G.D.; Zetts, S.P.; Pradhan, N. Phase Behavior in Systems Containing Clathrate Hydrates: A Review. *Rev. Chem. Eng.* **1988**, *5*, 1–70. [CrossRef]
62. Klauda, J.B.; Sandler, S.I. Modeling Gas Hydrate Phase Equilibria in Laboratory and Natural Porous Media. *Ind. Eng. Chem. Res.* **2001**, *40*, 4197–4208. [CrossRef]
63. Dufal, S.; Galindo, A.; Jackson, G.; Haslam, A.J. Modelling the Effect of Methanol, Glycol Inhibitors and Electrolytes on the Equilibrium Stability of Hydrates with the SAFT-VR Approach. *Mol. Phys.* **2012**, *110*, 1223–1240. [CrossRef]
64. El Meragawi, S.; Diamantonis, N.I.; Tsimpanogiannis, I.N.; Economou, I.G. Hydrate—Fluid Phase Equilibria Modeling Using PC-SAFT and Peng–Robinson Equations of State. *Fluid Phase Equilib.* **2016**, *413*, 209–219. [CrossRef]
65. Englezos, P. Clathrate Hydrates. *Ind. Eng. Chem. Res.* **1993**, *32*, 1251–1274. [CrossRef]
66. Ballard, A.L.; Sloan, E.D. The next Generation of Hydrate Prediction I. Hydrate Standard States and Incorporation of Spectroscopy. *Fluid Phase Equilib.* **2002**, *194–197*, 371–383. [CrossRef]
67. Jager, M.D.; Ballard, A.L.; Sloan, E.D. The next Generation of Hydrate Prediction: II. Dedicated Aqueous Phase Fugacity Model for Hydrate Prediction. *Fluid Phase Equilib.* **2003**, *211*, 85–107. [CrossRef]
68. Ballard, A.L.; Sloan, E.D. The next Generation of Hydrate Prediction Part III. Gibbs Energy Minimization Formalism. *Fluid Phase Equilib.* **2004**, *218*, 15–31. [CrossRef]
69. Vinš, V.; Jäger, A.; Span, R.; Hrubý, J. Model for Gas Hydrates Applied to CCS Systems Part I. Parameter Study of the van der Waals and Platteeuw Model. *Fluid Phase Equilib.* **2016**, *427*, 268–281. [CrossRef]
70. Vinš, V.; Jäger, A.; Hrubý, J.; Span, R. Model for Gas Hydrates Applied to CCS Systems Part II. Fitting of Parameters for Models of Hydrates of Pure Gases. *Fluid Phase Equilib.* **2017**, *435*, 104–117. [CrossRef]
71. Li, X.S.; Wu, H.J.; Englezos, P. Prediction of Gas Hydrate Formation Conditions in the Presence of Methanol, Glycerol, Ethylene Glycol, and Triethylene Glycol with the Statistical Associating Fluid Theory Equation of State. *Ind. Eng. Chem. Res.* **2006**, *45*, 2131–2137. [CrossRef]
72. Paricaud, P. Modeling the Dissociation Conditions of Salt Hydrates and Gas Semiclathrate Hydrates: Application to Lithium Bromide, Hydrogen Iodide, and Tetra-n-Butylammonium Bromide + Carbon Dioxide Systems. *J. Phys. Chem. B* **2011**, *115*, 288–299. [CrossRef]
73. Medeiros, F.D.A.; Segtovich, I.S.V.; Tavares, F.W.; Sum, A.K. Sixty Years of the van Der Waals and Platteeuw Model for Clathrate Hydrates—A Critical Review from Its Statistical Thermodynamic Basis to Its Extensions and Applications. *Chem. Rev.* **2020**, *120*, 13349–13381. [CrossRef] [PubMed]
74. Khan, M.N.; Warrier, P.; Peters, C.J.; Koh, C.A. Advancements in Hydrate Phase Equilibria and Modeling of Gas Hydrates Systems. *Fluid Phase Equilib.* **2018**, *463*, 48–61. [CrossRef]
75. Llamedo, M.; Anderson, R.; Tohidi, B. Thermodynamic Prediction of Clathrate Hydrate Dissociation Conditions in Mesoporous Media. *Am. Mineral.* **2004**, *89*, 1264–1270. [CrossRef]
76. Lipenkov, V.Y.; Istomin, V.A. On the Stability of Air Clathrate-Hydrate Crystals in Subglacial Lake Vostok, Antarctica. *Mater. Glyatsiol. Issled.* **2001**, *91*, 138–149.
77. McKay, C.P.; Hand, K.P.; Doran, P.T.; Andersen, D.T.; Priscu, J.C. Clathrate Formation and the Fate of Noble and Biologically Useful Gases in Lake Vostok, Antarctica. *Geophys. Res. Lett.* **2003**, *30*, 1702. [CrossRef]
78. Hand, K.P.; Chyba, C.F.; Carlson, R.W.; Cooper, J.F. Clathrate Hydrates of Oxidants in the Ice Shell of Europa. *Astrobiology* **2006**, *6*, 463–482. [CrossRef]
79. Thomas, C.; Mousis, O.; Picaud, S.; Ballenegger, V. Variability of the Methane Trapping in Martian Subsurface Clathrate Hydrates. *Planet Space Sci.* **2009**, *57*, 42–47. [CrossRef]
80. Tsimpanogiannis, I.N.; Thomas, D.; Economou, I.G.; Stubos, A.K. Evaluation of a Simple Model for Hydrate Equilibrium Calculations of Binary Gas Hydrates with Application to Gas-Mixture Separation. In Proceedings of the 8th International Conference on Gas Hydrates (ICGH8), Beijing, China, 28 July 2014.
81. Song, K.Y.; Kobayashi, R. The Water Content of Ethane, Propane and Their Mixtures in Equilibrium with Liquid Water or Hydrates. *Fluid Phase Equilib.* **1994**, *95*, 281–298. [CrossRef]
82. Von Stackelberg, M. Solid Gas Hydrates. *Naturwissenschaften* **1949**, *36*, 327–359.
83. Diepen, G.A.M.; Scheffer, F.E.C. The Ethene-Water System. *Recl. Trav. Chim. Pays-Bas* **2010**, *69*, 593–603. [CrossRef]

84. Reamer, H.H.; Selleck, F.T.; Sage, B.H. Some Properties of Mixed Paraffinic and Olefinic Hydrates. *J. Pet. Technol.* **1952**, *4*, 197–202. [CrossRef]
85. Sugahara, T.; Morita, K.; Ohgaki, K. Stability Boundaries and Small Hydrate-Cage Occupancy of Ethylene Hydrate System. *Chem. Eng. Sci.* **2000**, *55*, 6015–6020. [CrossRef]
86. Kubota, H.; Shimizu, K.; Tanaka, Y.; Makita, T. Thermodynamic Properties of R13 ($CClF_3$), R23 (CHF_3), R152a ($C_2H_4F_2$), and Propane Hydrates for Desalination of Sea Water. *J. Chem. Eng. Jpn.* **1984**, *17*, 423–429. [CrossRef]
87. Mooijer-van den Heuvel, M.M. Phase Behaviour and Structural Aspects of Ternary Clathrate Hydrate Systems: The Role of Additives. Ph.D. Thesis, Delft University of Technology, Delft, The Netherlands, 2004.
88. Mohammadi, A.H.; Anderson, R.; Tohidi, B. Carbon Monoxide Clathrate Hydrates: Equilibrium Data and Thermodynamic Modeling. *AIChE J.* **2005**, *51*, 2825–2833. [CrossRef]
89. Miller, S.L. Clathrate Hydrates of Air in Antarctic Ice. *Science* **1969**, *165*, 489–490. [CrossRef] [PubMed]
90. van Cleeff, A.; Diepen, G.A.M. Gas Hydrates of Nitrogen and Oxygen. II. *Recl. Trav. Chim. Pays-Bas* **1965**, *84*, 1085–1093. [CrossRef]
91. Mohammadi, A.H.; Richon, D. Ice−Clathrate Hydrate−Gas Phase Equilibria for Air, Oxygen, Nitrogen, Carbon Monoxide, Methane, or Ethane + Water System. *Ind. Eng. Chem. Res.* **2010**, *49*, 3976–3979. [CrossRef]
92. Mohammadi, A.H.; Tohidi, B.; Burgass, R.W. Equilibrium Data and Thermodynamic Modeling of Nitrogen, Oxygen, and Air Clathrate Hydrates. *J. Chem. Eng. Data* **2003**, *48*, 612–616. [CrossRef]
93. Byk, S.S.; Fomina, V.I. Gas Hydrates. *Russ. Chem. Rev.* **1968**, *37*, 469–491. [CrossRef]
94. Tamman, G.; Krige, G.J. Equilibrium pressures of gas hydrates. *Zeit. Anorg. Und Algem. Chem.* **1925**, *146*, 179–195.
95. Schroeder, W. Die Geschichte Der Gas Hydrate. *Sammlung. Chem. Tech. Vortrage* **1927**, *29*, 90–98.
96. Dyadin, Y.A.; Larionov, E.G.; Manakov, A.Y.; Zhurko, F.V.; Aladko, E.Y.; Mikina, T.V.; Komarov, V.Y. Clathrate Hydrates of Hydrogen and Neon. *Mendeleev Commun.* **1999**, *9*, 209–210. [CrossRef]
97. Kastanidis, P.; Tsimpanogiannis, I.N.; Romanos, G.E.; Stubos, A.K.; Economou, I.G. Recent Advances in Experimental Measurements of Mixed-Gas Three-Phase Hydrate Equilibria for Gas Mixture Separation and Energy-Related Applications. *J. Chem. Eng. Data* **2019**, *64*, 4991–5016. [CrossRef]
98. Olsen, B.; Majumdar, A.; Bishnoi, R. Experimental Studies Dioxide on Hydrate and Its Systems. *Int. J. Mat. Eng. Resour.* **1999**, *7*, 17–23.
99. Seo, Y.-T.; Kang, S.-P.; Lee, H.; Lee, C.-S.; Sung, W.-M. Hydrate Phase Equilibria for Gas Mixtures Containing Carbon Dioxide: A Proof-of-Concept to Carbon Dioxide Recovery from Multicomponent Gas Stream. *Korean J. Chem. Eng.* **2000**, *17*, 659–667. [CrossRef]
100. Kang, S.P.; Lee, H.; Lee, C.S.; Sung, W.M. Hydrate Phase Equilibria of the Guest Mixtures Containing CO_2, N_2 and Tetrahydrofuran. *Fluid Phase Equilib.* **2001**, *185*, 101–109. [CrossRef]
101. Linga, P.; Kumar, R.; Englezos, P. The Clathrate Hydrate Process for Post and Pre-Combustion Capture of Carbon Dioxide. *J. Hazard. Mater.* **2007**, *149*, 625–629. [CrossRef]
102. Bruusgaard, H.; Beltra, J.G.; Servio, P. Vapor-Liquid Water-Hydrate Equilibrium Data for the System N_2 + CO_2 + H_2O. *J. Chem. Eng. Data* **2008**, *53*, 2594–2597. [CrossRef]
103. Herri, J.M.; Bouchemoua, A.; Kwaterski, M.; Fezoua, A.; Ouabbas, Y.; Cameirao, A. Gas Hydrate Equilibria for CO_2-N_2 and CO_2-CH_4 Gas Mixtures-Experimental Studies and Thermodynamic Modelling. *Fluid Phase Equilib.* **2011**, *301*, 171–190. [CrossRef]
104. Belandria, V.; Eslamimanesh, A.; Mohammadi, A.; Richon, D. Gas Hydrate Formation in Carbon Dioxide + Nitrogen + Water System: Compositional Analysis of Equilibrium Phases. *Ind. Eng. Chem. Res.* **2011**, *50*, 4722–4730. [CrossRef]
105. Lang, F.; Servio, P. Solubility Measurements for the N_2 + CO_2 + H_2O System under Hydrate–Liquid–Vapor Equilibrium. *J. Chem. Eng. Data* **2014**, *59*, 2547–2550. [CrossRef]
106. Le Quang, D.; Le Quang, D.; Bouillot, B.; Herri, J.M.; Glenat, P.; Duchet-Suchaux, P. Experimental Procedure and Results to Measure the Composition of Gas Hydrate, during Crystallization and at Equilibrium, from N_2-CO_2-CH_4-C_2H_6-C_3H_8-C_4H_{10} Gas Mixtures. *Fluid Phase Equilib.* **2016**, *413*, 10–21. [CrossRef]
107. Jarrahian, A.; Nakhaee, A. Hydrate–Liquid–Vapor Equilibrium Condition of N_2 + CO_2 + H_2O System: Measurement and Modeling. *Fuel* **2019**, *237*, 769–774. [CrossRef]
108. Fan, S.-S.; Guo, T.-M. Hydrate Formation of CO_2-Rich Binary and Quaternary Gas Mixtures in Aqueous Sodium Chloride Solutions. *J. Chem. Eng. Data* **1999**, *44*, 829–832. [CrossRef]
109. Kim, S.H.; Seo, M.D.; Kang, J.W.; Lee, C.S. Hydrate-Containing Phase Equilibria for Mixed Guests of Carbon Dioxide and Nitrogen. *Fluid Phase Equilib.* **2011**, *306*, 229–233. [CrossRef]
110. Sfaxi, I.B.A.; Belandria, V.; Mohammadi, A.H.; Lugo, R.; Richon, D. Phase Equilibria of CO_2 + N_2 and CO_2 + CH_4 Clathrate Hydrates: Experimental Measurements and Thermodynamic Modelling. *Chem. Eng. Sci.* **2012**, *84*, 602–611. [CrossRef]
111. Lee, Y.; Lee, S.; Lee, J.; Seo, Y. Structure Identification and Dissociation Enthalpy Measurements of the CO_2 + N_2 Hydrates for Their Application to CO_2 Capture and Storage. *Chem. Eng. J.* **2014**, *246*, 20–26. [CrossRef]
112. Chapoy, A.; Burgass, R.; Tohidi, B.; Alsiyabi, I. Hydrate and Phase Behavior Modeling in CO_2-Rich Pipelines. *J. Chem. Eng. Data* **2015**, *60*, 447–453. [CrossRef]
113. Du, J.; Wang, L. Phase Equilibrium Measurements for Clathrate Hydrates of Flue Gas (CO_2 + N_2 + O_2) in the Presence of Tetra-n-Butyl Ammonium Bromide or Tri-n-Butylphosphine Oxide. *J. Chem. Thermodyn.* **2015**, *88*, 96–100. [CrossRef]

114. Lee, Y.; Lee, D.; Lee, J.W.; Seo, Y. Enclathration of CO_2 as a Co-Guest of Structure H Hydrates and its Implications for CO_2 Capture and Sequestration. *Appl. Energy* **2016**, *163*, 51–59. [CrossRef]
115. Sadeq, D.; Iglauer, S.; Lebedev, M.; Smith, C.; Barifcani, A. Experimental Determination of Hydrate Phase Equilibrium for Different Gas Mixtures Containing Methane, Carbon Dioxide and Nitrogen with Motor Current Measurements. *J. Nat. Gas. Sci. Eng.* **2017**, *38*, 59–73. [CrossRef]
116. Chazallon, B.; Pirim, C. Selectivity and CO_2 Capture Efficiency in CO_2-N_2 Clathrate Hydrates Investigated by in-Situ Raman Spectroscopy. *Chem. Eng. J.* **2018**, *342*, 171–183. [CrossRef]
117. Legoix, L.; Ruffine, L.; Deusner, C.; Haeckel, M. Experimental Study of Mixed Gas Hydrates from Gas Feed Containing CH_4, CO_2 and N_2: Phase Equilibrium in the Presence of Excess Water and Gas Exchange. *Energies* **2018**, *11*, 1984. [CrossRef]
118. Rho, W.G.; Kim, S.H.; Cho, D.-W.; Kang, J.W.; Lee, C.S. An Experimental and Modeling Study on Incipient Hydrate-Forming Conditions for Ternary Guests of Carbon Dioxide, Nitrogen and Sulfur Dioxide. *Fluid Phase Equilib.* **2018**, *473*, 127–131. [CrossRef]
119. Sugahara, T.; Murayama, S.; Hashimoto, S.; Ohgaki, K. Phase Equilibria for H_2 + CO_2 + H_2O System Containing Gas Hydrates. *Fluid Phase Equilib.* **2005**, *233*, 190–193. [CrossRef]
120. Kumar, R.; Wu, H.; Englezos, P. Incipient Hydrate Phase Equilibrium for Gas Mixtures Containing Hydrogen, Carbon Dioxide and Propane. *Fluid Phase Equilib.* **2006**, *244*, 167–171. [CrossRef]
121. Belandria, V.; Eslamimanesh, A.; Mohammadi, A.H.; Richon, D. Study of Gas Hydrate Formation in the Carbon Dioxide + Hydrogen + Water Systems: Compositional Analysis of the Gas Phase. *Ind. Eng. Chem. Res.* **2011**, *50*, 6455–6459. [CrossRef]
122. Linga, P.; Kumar, R.; Englezos, P. Gas Hydrate Formation from Hydrogen/Carbon Dioxide and Nitrogen/Carbon Dioxide Gas Mixtures. *Chem. Eng. Sci.* **2007**, *62*, 4268–4276. [CrossRef]
123. Chapoy, A.; Burgass, R.; Tohidi, B.; Austell, J.; Eickhoff, C. Effect of Common Impurities on the Phase Behavior of Carbon-Dioxide-Rich Systems: Minimizing the Risk of Hydrate Formation and Two-Phase Flow. *SPE J.* **2011**, *16*, 921–930. [CrossRef]
124. Bouchafaa, W.; Dalmazzone, D.; Victor, B. Thermodynamic Equilibrium Data for Mixed Hydrates of CO_2-N_2, CO_2-CH_4 and CO_2-H_2 in Pure Water and TBAB Solutions. École Nationale Supérieure de Techniques Avancées Unité Chime et Procédés. In Proceedings of the 7th International Conference on Gas Hydrates (ICGH 2011), Edinburgh, UK, 17–21 July 2011.
125. Pang, J.; Ng, H.J.; Zuo, J.; Zhang, D.; Ma, Q.; Chen, G. Hydrogen Gas Hydrate-Measurements and Predictions. *Fluid Phase Equilib.* **2012**, *316*, 6–10. [CrossRef]
126. Kang, S.P.; Lee, J.; Seo, Y. Pre-Combustion Capture of CO_2 by Gas Hydrate Formation in Silica Gel Pore Structure. *Chem. Eng. J.* **2013**, *218*, 126–132. [CrossRef]
127. Mohammadi, A.H.; Eslamimanesh, A.; Richon, D. Semi-Clathrate Hydrate Phase Equilibrium Measurements for the CO_2+H_2/CH_4+tetra-n-Butylammonium Bromide Aqueous Solution System. *Chem. Eng. Sci.* **2013**, *94*, 284–290. [CrossRef]
128. Xia, Z.; Li, X.; Chen, Z.; Li, G.; Wang, Y.; Jing, C.; Li, Z.; Lv, Q. Hydrate-Based Synchronously Capture of CO_2 and H_2S for Clean H_2 with New Synergic Additives. *Energy Procedia* **2017**, *142*, 3427–3432. [CrossRef]
129. Lee, W.; Kim, Y.-S.; Kang, S.-P. Semiclathrate-Based CO_2 Capture from Fuel Gas in the Presence of Tetra-n-Butyl Ammonium Bromide and Silica Gel Pore Structure. *Chem. Eng. J.* **2018**, *331*, 1–7. [CrossRef]
130. Unruh, C.H.; Katz, D.L. Gas Hydrates of Carbon Dioxide-Methane Mixtures. *J. Pet. Technol.* **1949**, *1*, 83–86. [CrossRef]
131. Adisasmito, S.; Frank, R.J.; Sloan, E.D. Hydrates of Carbon-Dioxide and Methane Mixtures. *J. Chem. Eng. Data* **1991**, *36*, 68–71. [CrossRef]
132. Ohgaki, K.; Takano, K.; Sangawa, H.; Matsubara, T.; Nakano, S. Methane Exploitation by Carbon Dioxide from Gas Hydrates. Phase Equilibria for CO_2-CH_4 Mixed Hydrate System. *J. Chem. Eng. Jpn.* **1996**, *29*, 478–483. [CrossRef]
133. Dholabhai, P.D.; Parent, J.S.; Bishnoi, P.R. Equilibrium Conditions for Hydrate Formation from Binary Mixtures of Methane and Carbon Dioxide in the Presence of Electrolytes, Methanol and Ethylene Glycol. *Fluid Phase Equilib.* **1997**, *141*, 235–246. [CrossRef]
134. Servio, P.; Lagers, F.; Peters, C.; Englezos, P. Gas Hydrate Phase Equilibrium in the System Methane–Carbon Dioxide–Neohexane and Water. *Fluid Phase Equilib.* **1999**, *158–160*, 795–800. [CrossRef]
135. Seo, Y.T.; Lee, H. Hydrate Phase Equilibria of the Carbon Dioxide, Methane, and Water System. *J. Chem. Eng. Data* **2001**, *46*, 381–384. [CrossRef]
136. Beltrán, J.G.; Servio, P. Equilibrium Studies for the System Methane + Carbon Dioxide + Neohexane + Water. *J. Chem. Eng. Data* **2008**, *53*, 1745–1749. [CrossRef]
137. Bruusgaard, H.; Beltrán, J.G.; Servio, P. Solubility Measurements for the CH_4 + CO_2 + H_2O System under Hydrate–Liquid–Vapor Equilibrium. *Fluid Phase Equilib.* **2010**, *296*, 106–109. [CrossRef]
138. Belandria, V.; Eslamimanesh, A.; Mohammadi, A.H.; Theveneau, P.; Legendre, H.; Richon, D. Compositional Analysis and Hydrate Dissociation Conditions Measurements for Carbon Dioxide plus Methane plus Water System. *Ind. Eng. Chem. Res.* **2011**, *50*, 5783–5794. [CrossRef]
139. Xia, Z.; Chen, Z.; Li, X.; Zhang, Y.; Yan, K.; Lv, Q.; Xu, C.; Cai, J. Thermodynamic Equilibrium Conditions for Simulated Land Fi Ll Gas Hydrate Formation in Aqueous Solutions of Additives. *J. Chem. Eng. Data.* **2012**, *57*, 3290–3295. [CrossRef]
140. Lee, S.; Park, S.; Lee, Y.; Seo, Y. Thermodynamic and 13C NMR Spectroscopic Verification of Methane-Carbon Dioxide Replacement in Natural Gas Hydrates. *Chem. Eng. J.* **2013**, *225*, 636–640. [CrossRef]
141. Bi, Y.; Yang, T.; Guo, K. Determination of the Upper-Quadruple-Phase Equilibrium Region for Carbon Dioxide and Methane Mixed Gas Hydrates. *J. Pet. Sci. Eng.* **2013**, *101*, 62–67. [CrossRef]

142. Xia, Z.; Li, X.; Chen, Z.; Li, G.; Cai, J.; Wang, Y.; Yan, K.; Xu, C. Hydrate-Based Acidic Gases Capture for Clean Methane with New Synergic. *Appl. Energy* **2017**, *207*, 584–593. [CrossRef]
143. Kastanidis, P.; Romanos, G.E.; Stubos, A.K.; Economou, I.G.; Tsimpanogiannis, I.N. Two- and Three-Phase Equilibrium Experimental Measurements for the Ternary CH_4 + CO_2 + H_2O Mixture. *Fluid Phase Equilib.* **2017**, *451*, 96–105. [CrossRef]
144. Seo, Y.T.; Lee, H. Multiple-Phase Hydrate Equilibria of the Ternary Carbon Dioxide, Methane, and Water Mixtures. *J. Phys. Chem. B* **2001**, *105*, 10084–10090. [CrossRef]
145. Belandria, V.; Mohammadi, A.H.; Richon, D. Phase Equilibria of Clathrate Hydrates of Methane+Carbon Dioxide: New Experimental Data and Predictions. *Fluid Phase Equilib.* **2010**, *296*, 60–65. [CrossRef]
146. Lee, S.; Lee, Y.; Lee, J.; Lee, H.; Seo, Y. Experimental Verification of Methane-Carbon Dioxide Replacement in Natural Gas Hydrates Using a Differential Scanning Calorimeter. *Environ. Sci. Technol.* **2013**, *47*, 13184–13190. [CrossRef] [PubMed]
147. Shi, L.L.; Liang, D.Q.; Li, D.L. Phase Equilibrium Conditions for Simulated Landfill Gas Hydrate Formation in Aqueous Solutions of Tetrabutylammonium Nitrate. *J. Chem. Thermodyn.* **2014**, *68*, 322–326. [CrossRef]
148. Obanijesu, E.O.; Barifcani, A.; Pareek, V.K.; Tade, M.O. Experimental Study on Feasibility of H_2 and N_2 as Hydrate Inhibitors in Natural Gas Pipelines. *J. Chem. Eng. Data* **2014**, *59*, 3756–3766. [CrossRef]
149. Zhou, X.; Long, Z.; Liang, S.; He, Y.; Yi, L.; Li, D.; Liang, D. In Situ Raman Analysis on the Dissociation Behavior of Mixed CH_4–CO_2 Hydrates. *Energy Fuels* **2016**, *30*, 1279–1286. [CrossRef]
150. Zang, X.; Liang, D. Phase Equilibrium Data for Semiclathrate Hydrate of Synthesized Binary CO_2/CH_4 Gas Mixture in Tetra-n-Butylammonium Bromide Aqueous Solution. *J. Chem. Eng. Data* **2017**, *62*, 851–856. [CrossRef]
151. Legoix, L.; Ruffine, L.; Donval, J.-P.; Haeckel, M. Phase Equilibria of the CH_4-CO_2 Binary and the CH_4-CO_2-H_2O Ternary Mixtures in the Presence of a CO_2-Rich Liquid Phase. *Energies* **2017**, *10*, 2034. [CrossRef]
152. Lim, J.; Choi, W.; Mok, J.; Seo, Y. Clathrate-Based CO_2 Capture from CO_2-Rich Natural Gas and Biogas. *ACS Sustain. Chem. Eng.* **2018**, *6*, 5627–5635. [CrossRef]
153. Lang, F.; Servio, P. Bulk Liquid and Gas Mole Fraction Measurements during Hydrate Growth for the CH_4 + CO_2 + H_2O System. *J. Chem. Thermodyn.* **2018**, *117*, 113–118. [CrossRef]
154. Mu, L.; von Solms, N. Hydrate Thermal Dissociation Behavior and Dissociation Enthalpies in Methane-Carbon Dioxide Swapping Process. *J. Chem. Thermodyn.* **2018**, *117*, 33–42. [CrossRef]
155. Matsui, Y.; Ogura, Y.; Miyauchi, H.; Makino, T.; Sugahara, T.; Ohgaki, K. Isothermal Phase Equilibria for Binary Hydrate Systems of Carbon Dioxide + Ethane and Carbon Dioxide + Tetrafluoromethane. *J. Chem. Eng. Data* **2010**, *55*, 3297–3301. [CrossRef]
156. Adisasmito, S.; Sloan, E.D. Hydrates of Hydrocarbon Gases Containing Carbon Dioxide. *J. Chem. Eng. Data* **1992**, *37*, 343–349. [CrossRef]
157. Maghsoodloo Babakhani, S.; Bouillot, B.; Douzet, J.; Ho-Van, S.; Herri, J.M. PVTx Measurements of Mixed Clathrate Hydrates in Batch Conditions under Different Crystallization Rates: Influence on Equilibrium. *J. Chem. Thermodyn.* **2018**, *122*, 73–84. [CrossRef]
158. Kim, S.H.; Huh, C.; Kang, S.-G.; Kang, J.W.; Lee, C.S. Phase Equilibria Containing Gas Hydrate of Carbon Dioxide, Sulfur Dioxide, and Water Mixtures. *J. Chem. Eng. Data* **2013**, *58*, 1879–1882. [CrossRef]
159. Sun, C.Y.; Ma, C.F.; Chen, G.J.; Zhang, S.X. Experimental and Simulation of Single Equilibrium Stage Separation of (Methane + Hydrogen) Mixtures via Forming Hydrate. *Fluid Phase Equilib.* **2007**, *261*, 85–91. [CrossRef]
160. Ma, Q.-L.; Chen, G.-J.; Ma, C.-F.; Zhang, L.-W. Study of Vapor–Hydrate Two-Phase Equilibria. *Fluid Phase Equilib.* **2008**, *265*, 84–93. [CrossRef]
161. Zhang, S.X.; Chen, G.J.; Ma, C.F.; Yang, L.Y.; Guo, T.M. Hydrate Formation of Hydrogen + Hydrocarbon Gas Mixtures. *J. Chem. Eng. Data* **2000**, *45*, 908–911. [CrossRef]
162. Skiba, S.S.; Larionov, E.G.; Manakov, A.Y.; Kolesov, B.A.; Kosyakov, V.I. Investigation of Hydrate Formation in the System H_2-CH_4-H_2O at a Pressure up to 250 MPa. *J. Phys. Chem. B* **2007**, *111*, 11214–11220. [CrossRef]
163. Matsumoto, Y.; Grim, R.G.; Khan, N.M.; Sugahara, T.; Ohgaki, K.; Sloan, E.D.; Koh, C.A.; Sum, A.K. Investigating the Thermodynamic Stabilities of Hydrogen and Methane Binary Gas Hydrates. *J. Phys. Chem. C* **2014**, *118*, 3783–3788. [CrossRef]
164. Happel, J.; Hnatow, M.A.; Meyer, H. The Study of Separation of Nitrogen from Methane by Hydrate Formation Using a Novel Apparatus—Discussion. *Ann. N. Y. Acad. Sci.* **1994**, *715*, 425–429. [CrossRef]
165. Mei, D.; Liao, J.; Yang, J.; Guo, T. Experimental and Modeling Studies on the Hydrate Formation of a Methane+ Nitrogen Gas Mixture in the Presence of Aqueous Electrolyte Solutions. *Ind. Eng. Chem. Res.* **1996**, *35*, 4342–4347. [CrossRef]
166. Nixdorf, J.; Oellrich, L.R. Experimental Determination of Hydrate Equilibrium Conditions for Pure Gases, Binary and Ternary Mixtures and Natural Gases. *Fluid Phase Equilib.* **1997**, *139*, 325–333. [CrossRef]
167. Lee, J.W.; Kim, D.Y.; Lee, H. Phase Behavior and Structure Transition of the Mixed Methane and Nitrogen Hydrates. *Korean J. Chem. Eng.* **2006**, *23*, 299–302. [CrossRef]
168. Zhong, D.; Englezos, P. Methane Separation from Coal Mine Methane Gas by Tetra-n-Butyl Ammonium Bromide Semiclathrate Hydrate Formation. *Energy Fuels* **2012**, *26*, 2098–2106. [CrossRef]
169. Zhong, D.L.; Daraboina, N.; Englezos, P. Coal Mine Methane Gas Recovery by Hydrate Formation in a Fixed Bed of Silica Sand Particles. *Energy Fuels* **2013**, *27*, 4581–4588. [CrossRef]
170. Zhong, D.L.; Daraboina, N.; Englezos, P. Recovery of CH_4 from Coal Mine Model Gas Mixture (CH_4/N_2) by Hydrate Crystallization in the Presence of Cyclopentane. *Fuel* **2013**, *106*, 425–430. [CrossRef]

171. Zhong, D.; Sun, D.; Lu, Y.; Yan, J.; Wang, J. Adsorption−Hydrate Hybrid Process for Methane Separation from a $CH_4/N_2/O_2$ Gas Mixture Using Pulverized Coal Particles. *Ind. Eng. Chem. Res.* **2014**, *53*, 15738–15746. [CrossRef]
172. Lim, D.; Ro, H.; Seo, Y.; Seo, Y.; Lee, J.Y.; Kim, S.-J.; Lee, J.; Lee, H. Thermodynamic Stability and Guest Distribution of $CH_4/N_2/CO_2$ Mixed Hydrates for Methane Hydrate Production Using N_2/CO_2 Injection. *J. Chem. Thermodyn.* **2017**, *106*, 16–21. [CrossRef]
173. Lee, H.H.; Ahn, S.H.; Nam, B.U.; Kim, B.S.; Lee, G.W.; Moon, D.; Shin, H.J.; Han, K.W.; Yoon, J.H. Thermodynamic Stability, Spectroscopic Identification, and Gas Storage Capacity of CO_2-CH_4-N_2 Mixture Gas Hydrates: Implications for Landfill Gas Hydrates. *Environ. Sci. Technol.* **2012**, *46*, 4184–4190. [CrossRef]
174. Sabil, K.M.; Nasir, Q.; Partoon, B.; Seman, A.A. Measurement of H-L_W-V and Dissociation Enthalpy of Carbon Dioxide Rich Synthetic Natural Gas Mixtures. *J. Chem. Eng. Data* **2014**, *59*, 3502–3509. [CrossRef]
175. Seo, Y.; An, S.; Park, J.-W.; Kim, B.-S.; Komai, T.; Yoon, J.-H. Occupation and Release Behavior of Guest Molecules in CH_4, CO_2, N_2, and Acetone Mixture Hydrates: An in-Situ Study by Raman Spectroscopy. *Ind. Eng. Chem. Res.* **2014**, *53*, 6179–6184. [CrossRef]
176. Kakati, H.; Mandal, A.; Laik, S. Phase Stability and Kinetics of CH_4 + CO_2 + N_2 Hydrates in Synthetic Seawater and Aqueous Electrolyte Solutions of NaCl and $CaCl_2$. *J. Chem. Eng. Data* **2015**, *60*, 1835–1843. [CrossRef]
177. Sun, D.; Ripmeester, J.; Englezos, P. Phase Equilibria for the $CO_2/CH_4/N_2/H_2O$ System in the Hydrate Region under Conditions Relevant to Storage of CO_2 in Depleted Natural Gas Reservoirs. *J. Chem. Eng. Data* **2016**, *61*, 4061–4067. [CrossRef]
178. Sun, Y.-H.; Li, S.-L.; Zhang, G.-B.; Guo, W.; Zhu, Y.-H. Hydrate Phase Equilibrium of CH_4 + N_2 + CO_2 Gas Mixtures and Cage Occupancy Behaviors. *Ind. Eng. Chem. Res.* **2017**, *56*, 8133–8142. [CrossRef]
179. Zang, X.; Liang, D. Phase Equilibrium Data for the Hydrates of Synthesized Ternary $CH_4/CO_2/N_2$ Biogas Mixtures. *J. Chem. Eng. Data* **2018**, *63*, 197–201. [CrossRef]
180. Kwon, M.; Lee, J.; Lee, H. Temperature-Dependent Structural Transitions in Methane—Ethane Mixed Gas Hydrates. *J. Phys. Chem. C* **2014**, *118*, 28906–28913. [CrossRef]
181. Soltanimehr, S.; Javanmardi, J.; Nasrifar, K. Liquid Water–Hydrate–Vapor Equilibrium for Methane + Ethane Gas Mixtures: Application of Gas Hydrates for Separation. *J. Chem. Eng. Data* **2017**, *62*, 2143–2148. [CrossRef]
182. Song, K.Y.; Kobayashi, R. Final Hydrate Stability Conditions of a Methane and Propane Mixture in the Presence of Pure Water and Aqueous Solutions of Methanol and Ethylene Glycol. *Fluid Phase Equilib.* **1989**, *47*, 295–308. [CrossRef]
183. Smith, C.; Pack, D.; Barifcani, A. Propane, n-Butane and i-Butane Stabilization Effects on Methane Gas Hydrates. *J. Chem. Thermodyn.* **2017**, *115*, 293–301. [CrossRef]
184. Lee, S.; Lee, Y.; Park, S.; Kim, Y.; Cha, I.; Seo, Y. Stability Conditions and Guest Distribution of the Methane + Ethane + Propane Hydrates or Semiclathrates in the Presence of Tetrahydrofuran or Quaternary Ammonium Salts. *J. Chem. Thermodyn.* **2013**, *65*, 113–119. [CrossRef]
185. Holder, G.D.; Hand, J.H. Multiple-Phase Equilibria in Hydrates from Methane, Ethane, Propane and Water Mixtures. *AIChE J.* **1982**, *28*, 440–447. [CrossRef]
186. Babakhani, S.M.; Bouillot, B.; Douzet, J.; Herri, J.M. A New Approach of Studying Mixed Gas Hydrates Involving Propane at Non-Equilibrium Conditions and Final State: An Experimental Study and Modeling. *Chem. Eng. Sci.* **2018**, *179*, 150–160. [CrossRef]
187. Chen, L.; Lu, H.; Ripmeester, J.A. Dissociation Conditions and Raman Spectra of CO_2 + SO_2 and CO_2 + H_2S Hydrates. *Ind. Eng. Chem. Res.* **2015**, *54*, 5543–5549. [CrossRef]
188. Mohammadi, A.H.; Richon, D. Hydrate Phase Equilibria of Gaseous Mixtures of Methane + Carbon Dioxide + Hydrogen Sulfide. *Chem. Eng. Commun.* **2015**, *202*, 629–633. [CrossRef]
189. Ward, Z.T.; Marriott, R.A.; Sum, A.K.; Sloan, E.D.; Koh, C.A. Equilibrium Data of Gas Hydrates Containing Methane, Propane, and Hydrogen Sulfide. *J. Chem. Eng. Data* **2015**, *60*, 424–428. [CrossRef]
190. Ma, Q.L.; Chen, G.J.; Sun, C.Y. Vapor-Liquid-Liquid-Hydrate Phase Equilibrium Calculation for Multicomponent Systems Containing Hydrogen. *Fluid Phase Equilib.* **2013**, *338*, 87–94. [CrossRef]
191. Kuhs, W.F.; Klapproth, A.; Chazallon, B. Chemical Physics of Air Clathrate Hydrates. In Proceedings of the Physics of Ice Core Records, International Symposium on Physics of Ice Core Records, Shikotsukohan, Hokkaido, Japan, 14–17 September 1998; pp. 373–392.
192. Yasuda, K.; Oto, Y.; Shen, R.; Uchida, T.; Ohmura, R. Phase Equilibrium Condition Measurements in Nitrogen and Air Clathrate Hydrate Forming Systems at Temperatures below Freezing Point of Water. *J. Chem. Thermodyn.* **2013**, *67*, 143–147. [CrossRef]
193. Kastanidis, P.; Romanos, G.E.; Michalis, V.K.; Economou, I.G.; Stubos, A.K.; Tsimpanogiannis, I.N. Development of a Novel Experimental Apparatus for Hydrate Equilibrium Measurements. *Fluid Phase Equilib.* **2016**, *424*, 152–161. [CrossRef]
194. Servio, P.; Englezos, P. Effect of Temperature and Pressure on the Solubility of Carbon Dioxide in Water in the Presence of Gas Hydrate. *Fluid Phase Equilib.* **2001**, *190*, 127–134. [CrossRef]